Received: 2 April 2024 | Revised: 19 August 2024 | Accepted: 29 August 2024

DOI: 10.1002/joc.8618

RESEARCH ARTICLE

International Journal of Climatology RMetS

Improving drought monitoring using climate models with bias-corrected under Gaussian mixture probability models

Rubina Naz[1] | **Zulfiqar Ali**[1] | **Veysi Kartal**[2] | **Mohammed A. Alshahrani**[3] | **Shreefa O. Hilali**[4] | **Fathia Moh. Al Samman**[5]

[1]College of Statistical Sciences, University of the Punjab, Lahore, Pakistan

[2]Department of Civil Engineering, Faculty of Engineering, Fırat University, Elazig, Turkey

[3]Department of Mathematics, College of Sciences and Humanities, Prince Sattam Bin Abdulaziz University, Alkharj, Saudi Arabia

[4]Department of Mathematics, College of Sciences and Arts (Majardah), King Khalid University, Magardah, Saudi Arabia

[5]Department of Mathematics, College of Science, Northern Border University, Arar, Saudi Arabia

Correspondence
Zulfiqar Ali, College of Statistical Sciences, University of the Punjab, Lahore, Pakistan.
Email: zulfiqar.stat@pu.edu.pk

Abstract

Global climate models (GCMs) are extensively used to calculate standardized drought indices. However, inaccuracies in GCM simulations and uncertainties inherent in the standardization methodology limit the precision of drought evaluations. The objective of this research is to remove bias in GCMs for improving drought monitoring and assessment. Consequently, this article proposes a new framework for drought index under the ensemble of GCMs—Multi-Model Quantile Mapped Standardized Precipitation Index (MMQMSPI). In accordance of Standardized Precipitation Index (SPI), the second stage derives a new index by assessing the feasibility of parametric and nonparametric models during standardization. In the application, we used 18 GCMs from the Coupled Model Intercomparison Project Phase 6 (CMIP6) data of precipitation across 32 grid points within the Tibetan Plateau region. The comparative findings reveal that the integration of KCGMD is the most suitable choice compared to other best-fitted univariate distributions in both features of the proposed framework. In this research, we assess the implications of evaluating future patterns of drought for the years 2015–2100 using seven different time periods and three different future scenarios. Temporal behavior clearly shows monthly variations in the pattern of MMQMSPI, and these variations differ on each time scale, but a drastic change can be seen over the long term, i.e., extreme dry and wet conditions, with a higher probability in all scenarios.

KEYWORDS

bias correction, drought, global climate models, *K*-component Gaussian mixture distribution

1 | INTRODUCTION

Accurate assessment of future drought is essential under the prevailing conditions of climate change and warming (Cook et al., 2018; Hoylman et al., 2022). Global warming has significantly influenced overall climate patterns and the spatiotemporal distributions of natural disasters (Banholzer et al., 2014). Over the last few decades, the projected temperature increase is expected to fall within the range of 0.80–1.20°C, with an expected rise to 1.50°C between the years 2030–2052 (Masson-Delmotte et al., 2022). The probability of increased frequency and intensity of precipitation extremes due to global warming has been quantified (Li et al., 2021). Usually, low precipitation and high vapor pressure lead to soil moisture deficiencies, resulting in drought conditions. Drought has widespread adverse impacts on the socioeconomic system, agriculture, ecology and water

supply (Zhang et al., 2022). In contrast to other natural hazards, the assessment and forecasting of drought are difficult and requires complex statistical modelling framework.

In recent research, GCMs have been extensively used for assessing climate characteristics and future predictions drought (Danandeh Mehr et al., 2020; Jehanzaib et al., 2020; Khan et al., 2020; Shirmohammadi et al., 2024; Song et al., 2021; Yao et al., 2020). The GCMs work as primary instruments to examine how the climate has changed across various time periods. The Intergovernmental Panel on Climate Change (IPCC) employs supercomputing resources to numerically solve a set of equations representing the dynamics of the climate system (Gutiérrez et al., 2021). Under the World Climate Research Programme (WCRP), the Coupled Model Intercomparison Project was started in 1995 and is currently in its sixth phase (CMIP6). The objective of CMIP6 is to raise the horizontal resolution and enhance the emission scenario process, thereby increasing the accuracy of future predictions (Peng et al., 2023).

In climate modelling, uncertainties are inevitable and are often associated with the structure and parametrization of the GCMs. Therefore, the main challenge faced by many researchers is the bias (systematic errors) in GCM models (Adeyeri et al., 2023; Hagemann et al., 2011; Lalande et al., 2023; Nahar et al., 2017). In this regard, selecting the optimal GCM for each research region aids in lowering modelling uncertainty, producing more accurate future forecasts. To reduce the uncertainty in GCMs, many ensemble techniques have been developed by several researchers (Gholami et al., 2023). They manly include Pagowski et al. (2005), Zounemat-Kermani et al. (2021), Yoon and Kang (2023), Kassim (2020), Dong et al. (2021), Fan et al. (2022) and Basak et al. (2023). However, the large-scale climate parameters that these models represent perform poorly when it comes to simulating processes like rainfall–runoff. GCMs and the regional climate model (RCM) outputs show systematic biases compared to observations (Gaur et al., 2023). Various sources of these errors include convection parameterization, unresolved fine-scale orography, irrational large-scale variability and unpredictable internal variability that differs from observations. The outputs generated by the models statistically deviate from the data. This bias needs to be addressed in statistical downscaling. Here, the mean, variance, higher moment and all quantiles of distributions can be adjusted using a variety of bias correction techniques (Kheir et al., 2023). In literature, several downscaling techniques were developed by several researchers. For example, the Delta approach has been used to adjust the moments of model outputs with those of the data, and quantile mapping (QM) has been utilized for all quantiles (Rajulapati & Papalexiou, 2023). The QM, a bias reduction approach, yields precise findings (Song et al., 2022).

In previous work, several researchers have explored various methods of mapping based on probabilistic quantile functions (Enayati et al., 2021; Pastén-Zapata et al., 2020), nonparametric quantile (Rajulapati & Papalexiou, 2023) and quantile delta mapping (QDM) (Xavier et al., 2022) according to the climatic variable suitability. However, for accurate inference, the appropriate probability distribution model must be selected in order to execute QM. In literature, different marginal distributions such as exponential (Heo et al., 2019; Niranjan Kumar et al., 2022), gamma (Heo et al., 2019; Pastén-Zapata et al., 2020) and empirical (Seo & Ahn, 2023) have been used for QM, by employing the cumulative distribution function (CDF) of GCM outputs for a base period and its inverse function of observations. Recently several researchers have examined the efficiency of *K*-components Gaussian mixture probability models (K-CGMPM) on precipitation data (Ali et al., 2020a, 2020b). Shin et al. (2019) applied mixture distributions on precipitation data of RCM in their study. Further, Ali et al. (2021) used the K-CGMPM on precipitation data of GCMs. Other recent related work includes Batool et al. (2023), Ahmad et al. (2023) and Yousaf et al. (2023). Additionally, a considerable amount of literature has been published on the implications of K-CGMPM in varying disciplines. Example include Ohn and Lin (2023), Fesl et al. (2023) and Srivastava et al. (2023).

Although studies have recognized the importance of K-CGMPM, research has yet to investigate the implications and appropriation of K-CGMPM in statistical downscaling. This paper considers the implication of K-CGMPM as a downscaling procedure and enhancing the standardized module of drought index. This paper aims to contribute to the accurate assessment of future drought under GCMs by enhancing the standardized module of the drought index through the implementation of K-CGMPM as a downscaling procedure. The motivation behind the uses of K-CGMPM compared to a simple univariate distribution lies in its features, which includes multimodality, flexibility, handling complex data, robustness to outliers, capturing correlations, enhanced representation, adaptability to different shapes and clustering capability (Benaglia et al., 2010; Yuan et al., 2023; Zhang et al., 2021). The specific research questions of this study are as follows: (1) Does K-CGMPM outperform existing approaches in terms of better fitness? (2) How can standardized drought indices be effectively integrated in the presence of complex data?

The remaining paper is as follows: section 2 is material and methods. Section 3 explains propagation and

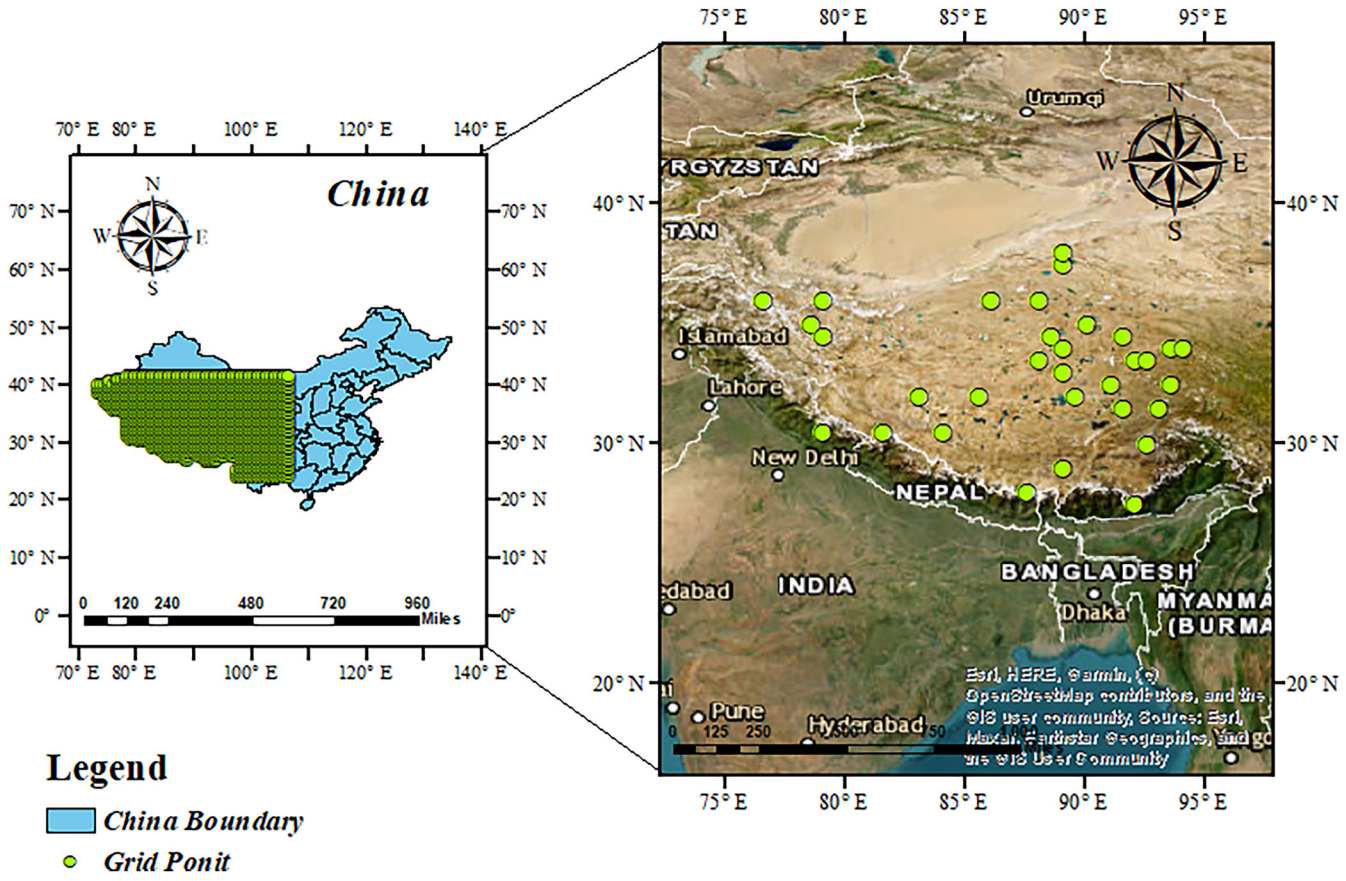

FIGURE 1 Spatial distribution of the selected grid points in the study region. [Colour figure can be viewed at wileyonlinelibrary.com]

implementation of the proposed bias correction procedure with the optimal procedure for the computation of drought indices. Section 4 consists on the results and discussion. Finally, section 7 presents the conclusion.

2 | MATERIALS AND METHODS

2.1 | Data and study area

This research is based on 32 grids points scattered around the Tibet Plateau region. Figure 1 shows the spatial distribution of grids points in the study region. The Tibet Plateau, also referred to as the Roof of the World, is a plateau that is scattered around 2.5 million square kilometers in size and is situated in Asia. At 4900 m above sea level, it is surrounded by the Karakoram Mountains to the north and the Himalayas to the south. Due to its regional importance, several researchers have assessed the spatiotemporal distributions of various climatic variables (Chen et al., 2022; Huang et al., 2022; Ma et al., 2022; Wang et al., 2022; Wei et al., 2022; Zhu et al., 2022a, 2022b). For this study, we used precipitation outputs of 18 CMIP6 models consisting the historical (1950–2014) and three future periods (2015–2100), namely SSP1-2.6, SSP2-4.5 and SSP5-8.5 (see Table 1). The future period includes three scenarios (SSP1-2.6, SSP2-4.5 and SSP5-8.5). This research uses a dataset of precipitation from multiple GCMs simulation from the CMIP6. The data set can be obtained from official website of World Climate Research Program. The detail description on the data set are available in Naz and Ali (2024) and Yousaf et al. (2023).

2.2 | Probability and non-probability (nonparametric) models

Probability models (univariate or multivariate) have various applications in several disciplines including hydrology (Anghel & Ilinca, 2022; Hipel & Fang, 2013). In past decades, univariate probability models have been extensively used in hydrological data (Shiau, 2020; Watterson, 2005). For example, Niranjan Kumar et al. (2022) have used the exponential distribution to model precipitation data. Similarly, two recent applications of the Gamma distribution include Pastén-Zapata et al. (2020) and Heo et al. (2019). Particularly in hydrology, the cumulative distribution function (CDF) of varying

TABLE 1 List of models along with modeling center of the 18 CMIP6 models.

S. No.	Model name	Modeling center
1	AWI-CM-1-1-MR	Alfred Wegener Institute, Helmholtz Centre for Polar and Marine Research, Germany
2	BCC-CSM2-MR	Beijing Climate Center and China Meteorological Administration, China
3	CanESM5	Canadian Centre for Climate Modeling and Analysis, Canada
4	CanESM5-CanOE	Canadian Centre for Climate Modeling and Analysis, Canada
5	ACCESS-CM2	Commonwealth Scientific and Industrial Research Organization, Australia
6	ACCESS-ESM1-5	Commonwealth Scientific and Industrial Research Organization, Australia
7	EC-Earth3-Veg	EC-Earth consortium, Europe
8	INM-CM4-8	Institute for Numerical Mathematics, Russia
9	INM-CM5-0	Institute for Numerical Mathematics, Russia
10	IPSL-CM6A-LR	Institute Pierre Simon Laplace, France
11	MPI-ESM1-2-LR	Max Planck Institute for Meteorology, Germany
12	UKESM1-0-LL	Met Office Hadley Centre, UK
13	HadGEM3-GC31-LL	Met Office Hadley Centre, UK
14	MRI-ESM2-0	Meteorological Research Institute, Japan
15	NESM3	Nanjing University of Information Science and Technology, China
16	CNRM-CM6-1	National Centre for Meteorological Research and European Centre for Research and Advanced Training in Scientific Computation, France
17	GFDL-ESM4	National Oceanic and Atmospheric Administration Geophysical Fluid Dynamics Laboratory, United States Computation, France
18	MIROC6	University of Tokyo, National Institute for Environmental Studies and Japan Agency for Marine-Earth Science and Technology, Japan

probability models and mixture of probability models for various regional data of precipitation are suggested to obtain SDI such as SPI and SPEI (Ali et al., 2017; Ali et al., 2020a, 2020b; Stagge et al., 2015). Huang et al. (2021) used a five-parameter Gamma-Gaussian model to normalize precipitation forecasts. In this research, we employed various well known multi parameters unimodal probability distributions to model the data using *propagate* package of R. Similarly, for bias correction procedure, several researchers used gamma and other identical probability model in bias correction procedure for GCMs ensemble data. Accordingly, Shin et al. (2019) used mixture probability distributions to precipitation data. In recent research, Ali et al. (2021) used the K-CGMD for GCMs in precipitation data. Though, several authors have developed numerous probabilistic functions for modeling random variables of various disciplines. Fitting an appropriate probability distribution on rainfall data plays important role for getting accurate Standardized Drought Index (SDI) (Erhardt & Czado, 2018). Parallel to the use of univariate probability functions, the mixture of Gaussian probability function is commonly used for modeling complex data (Ali et al., 2020a, 2020b). However, accurate probabilistic modelling requires a mixture of probability functions for complex data (Batool et al., 2023).

Many recent studies are based on mixture models with various distributions (An et al., 2022; Katsevich & Bandeira, 2023; Zhu et al., 2022a, 2022b). The use of the cumulative distribution function (CDF) of the mixture probability model reduces uncertainty and improves the accuracy of modeling (Ali et al., 2020a, 2020b). Following the approach of Ali et al. (2020a, 2020b) and Batool et al. (2023), we employ a mixture K-CGMD in both phases of the proposed framework. In case of appropriateness of uni-model probability function, we suggest to use K-CGMD. In this study, we employed the "mixtool" package (Benaglia et al., 2010) in R to estimate the parameters of K-CGMD. The mathematical expression of KCGMD is as follows:

$$P(y)\sum_{j=1}^{n}\beta_j N\left(y|\mu_j,\sigma_j\right), \tag{1}$$

$$N\left(y|\mu_j,\sigma_j\right)=\frac{1}{\sigma_{j\sqrt{2\pi}}}\exp\left(\frac{-\left(y-\mu_j\right)^2}{2\sigma_j^2}\right). \tag{2}$$

In the above equations, β_j denotes the weight of jth component with $\sum_{j=1}^{n}\beta_j=1$. β_j and σ_j denote mean and variance of jth component. KCGMD is useful for modeling complex data climate. In previous research, several authors have used KCGMD for modeling precipitation and temperature data (Ali et al., 2020a, 2020b; Ali et al., 2023; Batool et al., 2023).

In the proposed research, we proposed the implications of K-CGMD in bias correction procedure for GCMs ensemble. However, in the standardization of the bias corrected data, we incorporated both the probability and non-probability models to increase the generalization of the proposed framework. A brief description on nonparametric functions is given in the following section.

2.3 | Probability plotting position formula as a nonparametric approach for modeling variables

In statistics, nonparametric modeling plays an indispensable role (Manoukian, 2022). Nonparametric procedures serve as important tools for modeling complex data (Conover & Iman, 1981). This approach enables meaningful comparisons and facilitates drawing statistical conclusions without relying on specific distribution assumptions. It involves replacing the data with ranks, and in the case of ties, using average ranks before applying standard procedures to the ranks. Leys and Schumann (2010) used nonparametric tests involving ranked and adjusted rank transformations, demonstrating the superiority of these techniques over parametric tests through Monte Carlo simulations. Conover (2012) applied classical statistical procedures to both the actual data and its ranks, such as the t test and correlation coefficient, concluding their similarity in results. A straightforward technique to bridge the pedagogical gap between parametric and nonparametric statistical methods is the use of rank transformation.

In the literature, many nonprobability plotting position formulae, serving as a nonparametric alternative to probability distributions, are available. They mainly include Gringroten, Hazzan, Hirsch, Weibull, and so on. A list of probability plotting position formula is available in Ali et al. (2020a, 2020b).

In nonparametric modeling, the data are ranked, and the quantiles are used to estimate the cumulative distribution function (CDF). For example, in case of Gringroten formula, let, $X_i \in X_{1i}, X_{2i}, \ldots, X_{ni}$ be the GCMs of precipitation data at a location i. Then CDF can be defined as follows:

$$F(X)=(\text{Rank}(Fx_i)-0.5)/n, \tag{3}$$

where n represents the total number of GCMs.

In hydrology, Farahmand and AghaKouchak (2015) developed a framework of nonparametric drought indices based on Gringroten formula. In later research, Ali et al. (2020a, 2020b) suggests a new generalized formula by including multiple non parametric formulas. In this research, we use nonparametric approach when we failed to model the data using probability models ether univariate or multivariate. However, we employ either a univariate or nonparametric plotting position formula, where either has a single peak (unimodal) and can be modeled using a univariate probability function. The choice of using either K-CGMM or a univariate model is based on the Bayesian information criterion (BIC), Akaike information criterion (AIC) and second order Akaike information criterion (AICc).

2.4 | Simple average scheme

The ensemble value is derived as a weighted average of individual component outputs in the context of a simple average scheme (SAS). Each component is assigned an equal weight, resulting in the ensemble value being the arithmetic mean of the component outputs. SAS proves beneficial in enhancing the precision of climate simulations, particularly for variables influenced by multiple aspects of the climate system. It is important to note that SAS is just one among the various techniques employed in GCMs to enhance accuracy and reliability (Hausfather et al., 2020).

In the first step, the simple average method has been used to calculate the ensemble GCMs model provided in Table 1 with model name, center and resolution. Mathematically, let $X_i \in X_{1i}, X_{2i}, \ldots, X_{ni}$ be the GCMs of precipitation data at a location i. Let y_i be the observed vector of precipitation at a location i. Here, the main objective is to develop weights for the aggregation of multiple GCMs in such a way that all models receive equal weights. The following expression denotes the ensemble data,

$$\overline{X}=\frac{\sum X_i}{n}, \tag{4}$$

where n represents the total number of GCMs. Above equation has been used as ensemble model for bias correction.

2.5 | Bayesian information criterion as a model selection measures

Most often, the performance of the distributions is evaluated and investigated based on the Schwarz information

criterion, sometimes referred to as BIC. In this paper, BIC is applied to assess the model performance and complexity.

The mathematical and detailed description is available in Schwarz (1978). The lower value indicates a better-fitting model or distribution,

$$\mathrm{BIC} = -2\times(\log-\mathrm{likelihood}) + \log(n)\times k, \tag{5}$$

where n is the sample size and k is the number of model parameters. The lesser BIC suggests a better model.

Recently, many researchers have used BIC in their goodness of fit selection criteria. For example, Sung et al. (2022) applied BIC to access a better fit model based on daily, weekly and monthly data of drought. Jiang et al. (2023) used BIC in their research for estimating the hierarchical model of hydrological distribution. In addition to BIC, we included AIC and AICs for validating the findings. The following equations provide the mathematical formulations for AIC and AICc, respectively:

$$\mathrm{AIC} = 2K - 2\ln(\mathrm{likelihood}), \tag{6}$$

$$\mathrm{AIC}_c = \mathrm{AIC} + \frac{2K^2 - 2K}{n-K-1}. \tag{7}$$

3 | THE PROPOSED FRAMEWORK OF MULTI-MODEL QUANTILE MAPPED STANDARDIZED PRECIPITATION INDEX

This section provides the rational and the mathematical descriptions of the Multi-Model Quantile Mapped Standardized Precipitation Index (MMQMSPI).

The framework of MMQMSPI is divided into two stages (see Figure 2). The first stage provides a new way to integrate mixture of Gaussian probability models in bias correction of GCMs which results in more accurate future ensemble data of GCMs. Consequently, this stage provides a new bias correction procedure for GCMs.

While the second stage standardizes the ensemble data under an optimal standardization setting. This step is due to the statistical findings on the implications of unimodal probability functions (Ali et al., 2017; Stagge et al., 2015), multimodal mixture models (Ali et al., 2020a, 2020b) and nonparametric probability plotting position formula (Hao et al., 2018) in the standardization procedure of Standardized Drought Indices (SDI).

The detailed descriptions on both stage of the proposed framework is given in the following subsections.

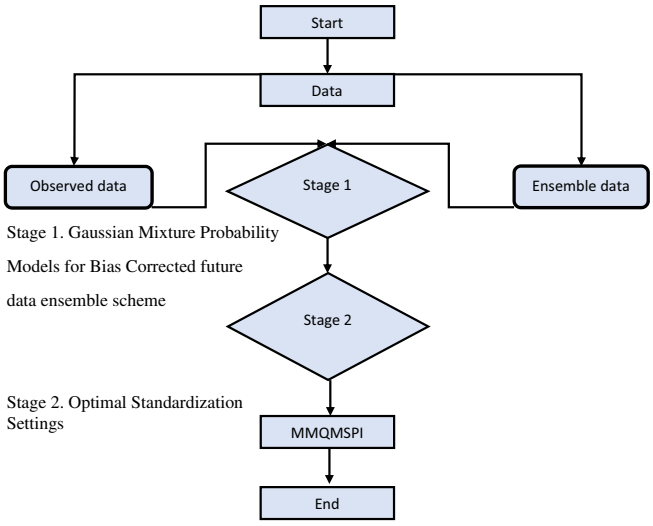

FIGURE 2 Flow chart of the proposed research framework. [Colour figure can be viewed at wileyonlinelibrary.com]

3.1 | Stage 1: Gaussian mixture probability models for bias-corrected future data ensemble scheme

GCM outputs cover the base and future, which are two separate periods. A base period indicates a simulation length that takes observable climatic conditions into account. The duration of the simulation that accounts for climatic forcing is presented as a future period. The statistical comparison between GCM outputs and observations is often used to validate future GCMs.

The first stage of MMQMSPI provides the rationale and scheme of using Gaussian mixture probability models for bias correction of future ensemble data.

Symbolically, let $x_{m,\mathrm{fut}}$, y_{obs} and $\widehat{y}_{m,\mathrm{fut}}$ denote future model data, observed data, bias-corrected future model data, respectively.

In QM, the relationship between the quantiles of a series of past GCM simulations and the data that matches them is used to modify a set of climatic predictions. The quantile connection is discovered by separately fitting the historical GCM simulations and data with CDF. The bias in the simulated data generated by a GCM (x) is removed by QM by converting quantiles between the simulated data and the observed data (y) sets at the same cumulative probability by matching the CDF, $F(x;\theta)$, where θ represents the parameter set values of the two distributions. Thus, the CDF of the GCM output data is transferred to the observed data. Here, the QM equation is shown as

$$\widehat{y} = {F_{\mathrm{obs}}}^{-1}(F_{m,\mathrm{base}}(x)), \tag{8}$$

where $F_{m,\text{base}}$ represents CDF of GCM model output for the base period and ${F_{\text{obs}}}^{-1}$ denotes the inverse function of CDF for historical model. However, the complicated structure of ensemble data limits the applicability of unimodal distributions. Consequently, a more sophisticated model is necessary to effectively represent ensemble data. In addressing this challenge, we propose the following procedure to derive bias-corrected future data from an ensemble of multiple GCMs. Let, Y_{obs}, Y_{enz}, Y_{fut}, $\widehat{y}_{\text{fut}}$ denote the observations in reference periods, the ensemble of multiple GCMs in the reference period, the ensemble of multiple GCMs in the future period and the bias-corrected (improved ensemble) of multiple GCMs in the future period. Then, the following steps are proposed to obtain bias-corrected future data from the ensemble of multiple GCMs.

i. The first step suggests to calculate the CDFs for observed data $(F(Y_{\text{obs}}))$ and for ensemble of GCMs data $(F(Y_{\text{enz}}))$ using K-CGMD.

In this research, we used 12 components of Gaussian mixture distribution and estimate the parameters using EM algorithm. The use of 12 component is due to the lemma of seasonality provided in Ali et al. (2020a, 2020b).

ii. The second step suggests to extract the parametric values of Y_{obs} and Y_{enz} as vectors of mean, $\alpha=\{\alpha_1,\alpha_2,\alpha_3,...,\alpha_{12}\}$ and variance $\beta=\{\beta_1,\beta_2,\beta_3,...,\beta_{12}\}$. The vectors of parametric combination and possible matching pairs at each step have been adjusted to better fit the corresponding category.

In this research, the parametric value less than or equal to zero is replaced by its mean value of the targeted data set.

iii. The third step calculates the quantiles of K-CGMD for F_{enz} by using shape and scale parameters of Y_{obs}.
iv. This step computes the CDF of K-CGMD for Y_{fut} by using shape and scale parameters of F_{enz} and named as F_{oef}.
v. This step generates quantiles of F_{oef} by using shape and scale parameters of Y_{obs} and compute bias correct future ensemble data $\widehat{y}_{\text{fut}}$.
vi. This step provides a weighting scheme proposed by Ali et al. (2017) for future aggregation of precipitation data based on divergence between bias corrected reference data $(\widehat{y})$ and future simulated GCMs data (M_i) where $i=1,2,...,k$.

Mathematically,

$$v=1-\frac{\exp^{\left|\widehat{y}-M_i\right|}}{\sum_{i=1}^{k}\exp^{\left|\widehat{y}-M_i\right|}}. \tag{9}$$

Further,

$$w_i=\frac{v_i}{\sum_{i=1}^{k}v_i}. \tag{10}$$

Subject to the condition that $\sum_{i=1}^{k}w_i=1$. Here, k represents the number of GCMs.

vii. This is the final step of the proposed bias correction procedure. The estimated weights from Equation (4) are suggested to average the time series data of GCMs. Mathematically,

$$\text{QMSD}_i=\sum_{i=1}^{k}M_iw_i. \tag{11}$$

In the above equation, QMSD_i represents weighted average of all the GCMs.

3.2 | Stage 2: Optimal standardization settings

This stage provides the descriptions on the second stage of the MMQMSPI. On the same lines of the recent work of Naz and Ali (2024), this stage suggests the optimal standardization of the ensemble data QMSD_i using either parametric or nonparametric based procedure.

Symbolically, let $\mathcal{E}$ and f denote the CDF of univariate probability models and mixture probability models. Let γ denotes quantile points of Weibull probability plotting position formula. Then we suggest the following two conditions of the optimal choice of CDF.

Condition 1:

If

$$\beta_{\mathcal{E}}<\beta_f, \tag{12}$$

use the CDF of appropriately selected univariate probability model, and if

Condition 2:

$$\beta_{\varepsilon} > \beta_{f}, \tag{13}$$

use the CDF of mixture probability models, and/otherwise; use the quantile points ϒ of Weibull probability plotting position as a CDF. In Equations (6) and (7), β represents the numerical values of Bayesian information criterion (BIC).

After the selection of appropriate data fitness methods, we standardize the corresponding CDF by employing the standardization approximation given by (Abramowitz & Stegun, 1968). We refer to the standardized data as MMQMPSI. Furthermore, the classification of drought intensity can be made according to the classification criterion provided by McKee et al. (1993).

The system of equations of the standardization is as follows:

$$\mathrm{MMQMPSI} = -\left(u + \frac{f_0 + f_1 u + f_2 u^2}{1 + h_1 u + h_2 u^2 + h u^3}\right), \tag{14}$$

for

TABLE 2 Drought classification criterion for SPI and MMQMSPI drought index.

Range of MMQMSPI	Classes
2.00 and above	Extremely Wet (EW)
1.50 to 1.99	Very Wet (VW)
1.00 to 1.49	Moderate Wet (MW)
−0.99 to 0.99	Near Normal (NN)
−1.00 to −1.49	Moderate Dry or Drought (MD)
−1.50 to −1.99	Severe Dry or Drought (SD)
−2.00 and less	Extremely Dry or Drought (ED)

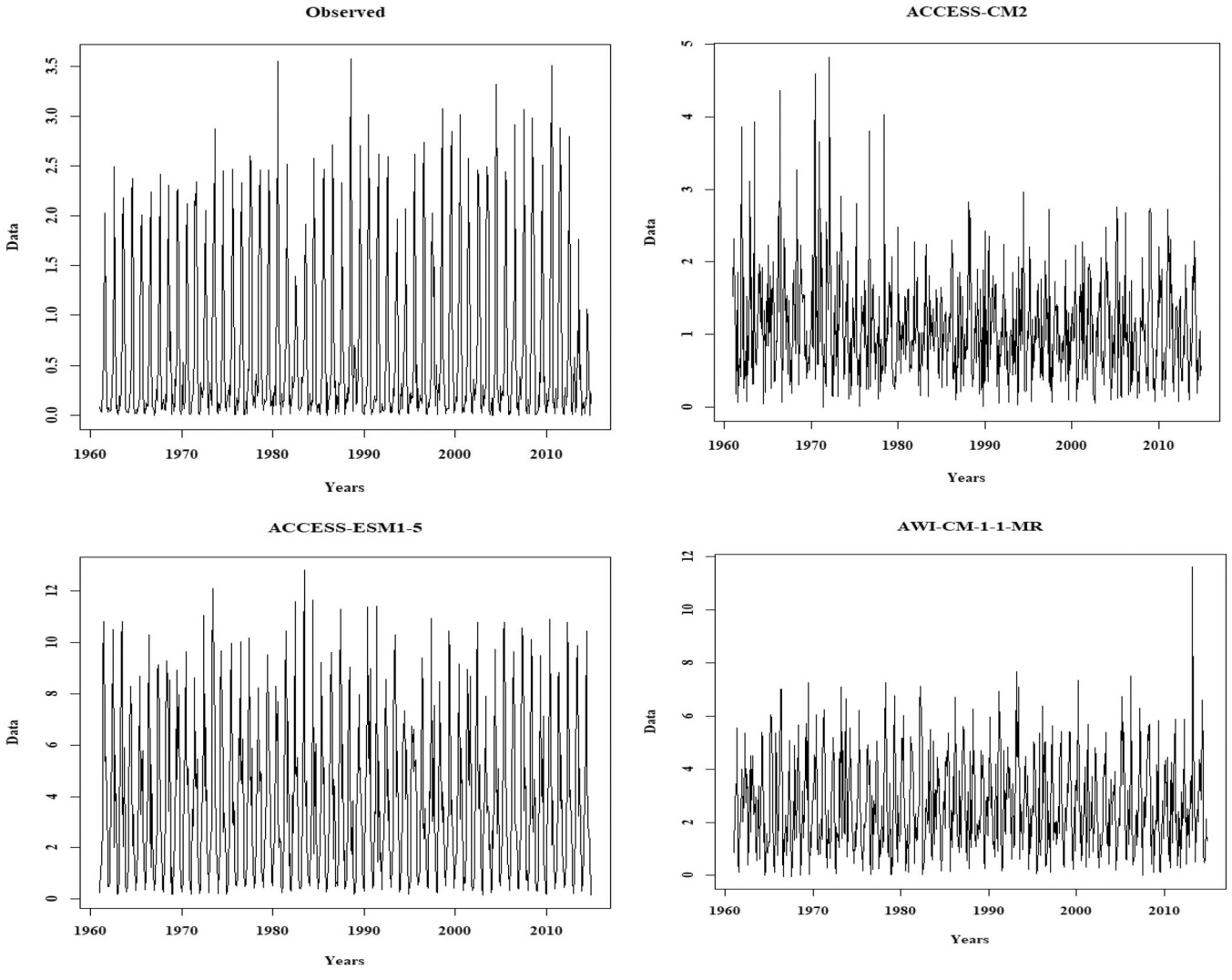

FIGURE 3 Observed and historical simulations (three models) of precipitation data of GCMs.

TABLE 3 BIC values of 32 various univariate probability models.

S. No.	Distribution	Observed	Ensemble	For MMQMSPI			For SPI		
				SSP1-2.6	SSP2-4.5	SSP5-8.5	SSP1-2.6	SSP2-4.5	SSP5-8.5
1	2P Beta	−167.993	−512.400	−62.512	−75.833	−68.776	134.5571	127.8761	104.2497
2	3P Weibull	−418.610	−654.688	−233.434	−206.085	−210.622	33.56838	11.41678	−13.4462
3	4P Beta	−357.218	−648.050	−162.766	−160.488	−203.749	15.38182	6.460054	−28.7807
4	Arcsine	−237.328	−588.165	−81.379	−92.874	−73.319	95.10814	101.8603	72.87255
5	Burr	−338.162	−524.071	−137.423	−143.960	−116.642	91.2869	65.86093	48.16708
6	Cauchy	−345.573	−664.393	−156.532	−168.295	−130.678	88.17431	60.86915	48.20519
7	Chi	−181.437	−517.534	−113.400	−117.439	−88.895	74.36022	49.04549	33.17598
8	Chi-Square	−356.236	−532.991	−158.962	−174.357	−135.112	98.99994	77.61239	56.83812
9	Cosine	−261.093	−589.426	−95.724	−103.440	−74.756	84.09086	57.88369	45.11884
10	Curvilinear Trapezoidal	−317.414	−624.814	−145.443	−151.246	−117.417	58.62602	28.94099	8.904466
11	Exponential	−369.170	−658.546	−160.273	−173.400	−133.931	86.52892	65.08934	39.72668
12	F-	−410.255	−584.485	−186.611	−198.873	−156.701	66.69591	31.65908	16.45447
13	Gamma	−364.472	−657.257	−155.417	−169.837	−130.772	71.92435	43.15542	22.6815
14	Generalized Extreme Value	−415.639	−731.602	−245.619	−256.473	−204.785	46.9887	16.35541	4.718796
15	Generalized normal	−430.499	−737.550	−251.502	−267.471	−215.297	37.41036	10.95415	−6.37177
16	Gumbel	−337.855	−645.085	−150.596	−160.996	−124.829	79.01702	51.04061	33.8755
17	Inverse Chi-Square	−393.909	−597.183	−215.368	−230.275	−178.620	99.8175	85.18383	56.23338
18	Inverse Gamma	−396.767	−698.495	−211.847	−225.438	−174.738	64.29242	30.66998	14.75058
19	Inverse Gaussian	−392.252	−695.494	−208.924	−224.336	−173.428	64.81542	32.75682	13.74601
20	Johnson SB	−441.157	−753.495	−267.339	−287.794	−240.329	−24.2959	−30.7996	−51.2336
21	Johnson SU	−425.687	−734.960	−250.101	−264.163	−211.987	42.14655	15.18907	−1.48138
22	Laplace	−350.468	−658.968	−165.200	−175.087	−135.313	82.004	53.223	39.65496
23	Logistic	−324.111	−643.047	−143.471	−152.881	−119.848	92.00489	66.70624	52.3922
24	Log-normal	−422.509	−674.737	−181.136	−195.375	−149.807	68.17046	37.36983	17.86583
25	Normal	−315.988	−638.550	−140.775	−148.562	−116.615	88.57964	63.00977	49.68568
26	Rayleigh	−324.335	−639.280	−145.569	−154.549	−120.243	79.52157	52.06856	36.26946
27	Scaled/shifted t-	−341.480	−663.855	−160.238	−167.783	−128.141	91.14066	67.86959	52.92385
28	Skewed-normal	−327.824	−635.801	−143.708	−153.393	−118.073	56.2666	25.20888	10.86458
29	Trapezoidal	−314.782	−620.000	−145.929	−160.958	−112.468	52.06871	17.89888	4.051843
30	Triangular	−314.484	−631.934	−148.438	−154.382	−117.088	44.38152	12.55021	−3.18831
31	Uniform	−153.818	−520.204	−112.670	−3.478	−85.582	188.7912	185.8987	102.1982
32	von Mises	−324.340	−530.611	−142.586	−151.476	−119.089	92.23449	67.24606	53.41578

$$u=\sqrt{\ln\left(\frac{1}{F(x)^2}\right)}, \tag{15}$$

when

$$0\le F(x)\le 0.5, \tag{16}$$

and

$$\mathrm{MMQMPI}=+\left(u+\frac{f_0+f_1u+f_2u^2}{1+h_1u+h_2u^2+h_3u^3}\right), \tag{17}$$

where

$$v=\sqrt{\ln\left(\frac{1}{\{1-F(x)\}^2}\right)}, \tag{18}$$

TABLE 4 AIC values of 32 various univariate probability models.

S. No.	Distribution	Observed	Ensemble	For MMQMSPI			For SPI		
				SSP1-2.6	SSP2-4.5	SSP5-8.5	SSP1-2.6	SSP2-4.5	SSP5-8.5
1	2P Beta	101.322	123.610	114.654	127.506	96.821	126.349	119.297	95.579
2	3P Weibull	42.293	25.829	−79.926	23.030	−124.964	22.624	−0.022	−25.008
3	4P Beta	45.030	21.371	−80.251	21.406	−144.090	1.701	−7.839	−43.233
4	Arcsine	226.757	99.735	99.507	113.384	75.295	86.900	93.281	64.202
5	Burr	297.779	91.363	73.374	86.965	19.126	85.815	60.141	42.386
6	Cauchy	25.176	78.056	−31.257	−0.006	−186.439	79.966	52.290	39.534
7	Chi	137.566	57.902	50.198	70.535	−23.392	68.888	43.326	27.395
8	Chi-Square	156.177	98.328	90.450	103.012	55.589	93.528	71.893	51.057
9	Cosine	274.845	69.075	24.100	71.119	−25.995	75.882	49.304	36.448
10	Curvilinear Trapezoidal	47.383	47.310	72.564	25.335	−107.431	47.681	17.502	−2.657
11	Exponential	80.024	81.525	93.421	107.144	68.451	81.057	59.370	33.946
12	F-	169.132	54.635	101.578	117.625	86.719	58.487	23.080	7.783
13	Gamma	70.561	56.568	−84.257	20.105	−138.667	63.716	34.576	14.010
14	Generalized Extreme Value	−43.196	43.221	−81.825	14.444	−172.546	36.044	4.916	−6.843
15	Generalized normal	−34.891	34.673	−82.266	16.776	−160.144	26.466	−0.485	−17.933
16	Gumbel	43.432	62.583	−75.465	14.644	−164.117	70.808	42.461	25.204
17	Inverse Chi-Square	294.140	93.533	100.946	114.900	79.895	94.345	79.464	50.453
18	Inverse Gamma	−9.993	50.076	−82.708	17.716	−152.883	56.084	22.091	6.080
19	Inverse Gaussian	6.469	50.045	−83.904	19.001	−145.130	56.607	24.177	5.075
20	Johnson SB	−32.891	−4.130	−80.267	18.777	−158.143	−37.977	−45.099	−65.685
21	Johnson SU	−40.660	36.631	−80.269	−16.638	−239.083	28.466	0.890	−15.933
22	Laplace	25.268	70.398	−47.119	−8.797	−191.092	73.795	44.644	30.984
23	Logistic	55.736	76.139	−77.907	17.109	−149.247	83.796	58.127	43.721
24	Log-normal	−17.419	53.032	−83.919	18.903	−145.872	59.962	28.790	9.195
25	Normal	66.186	73.131	−82.386	22.279	−125.842	80.371	54.430	41.015
26	Rayleigh	56.480	63.220	34.548	72.699	10.258	71.313	43.489	27.598
27	Scaled/shifted t-	26.948	75.131	−80.386	−8.545	−191.455	80.196	56.430	41.362
28	Skewed-normal	54.244	37.671	−81.978	18.657	−153.394	45.322	13.770	−0.697
29	Trapezoidal	73.965	45.817	−69.291	22.529	−128.897	38.388	3.600	−10.400
30	Triangular	72.636	27.277	−69.450	20.529	−130.893	33.437	1.111	−14.750
31	Uniform	281.807	122.499	111.297	96.976	58.606	180.583	177.319	93.527
32	von Mises	66.083	75.542	−82.364	21.868	−129.159	84.026	58.667	44.745

when

$$0.5 \leq F(x) \leq 1. \tag{19}$$

Also, the constants include $f_0 = 2.515517$, $f_1 = 0.802853$, $f_2 = 0.010328$, $h_1 = 1.432788$, $h_2 = 0.985269$, $h_3 = 0.001308$.

The main differences between SPI and MMQSMPI are (1) the use of a mixture probability model instead of a univariate probability distribution, (2) the use of ensemble data under the proposed weighting scheme presented in the stage 1 instead of equal ensemble data. However, the temporal vector of MMQMSPI and SPI can be categorized by the classification criterion given in Mckee et al. (1993). The drought classification criteria for the MMQMSPI index are shown in Table 2. The MMQMSPI drought index classes fall into the following ranges: Extremely Wet (EW) for 1.00 and above, Very Wet (VW) for 1.50–1.99, Moderate Wet (MW) for 1.00–1.49, Near Normal (NN) for −0.99 to 0.99, Moderate Drought (MD) for −1.00 to −1.49,

TABLE 5 AICc values of 32 various univariate probability models.

S. No.	Distribution	Observed	Ensemble	For MMQMSPI			For SPI		
				SSP1-2.6	SSP2-4.5	SSP5-8.5	SSP1-2.6	SSP2-4.5	SSP5-8.5
1	2P Beta	101.340	161.623	175.120	199.577	193.116	215.828	234.113	233.724
2	3P Weibull	42.330	31.895	−77.825	33.814	−122.603	48.471	4.859	−24.952
3	4P Beta	45.092	28.277	−78.600	32.400	−141.923	35.804	−5.191	−43.191
4	Arcsine	226.775	345.575	448.976	807.611	5921.977	−14256.100	26680.760	−55444.300
5	Burr	297.798	600.988	1756.057	−8424.070	15028.320	−32186.900	62433.930	−126924.000
6	Cauchy	25.195	80.178	−17.566	0.549	−186.437	136.761	94.427	58.776
7	Chi	137.572	132.745	89.729	87.833	−6.847	68.965	53.357	33.329
8	Chi-Square	156.183	198.362	185.440	184.788	136.730	135.644	113.295	79.278
9	Cosine	274.863	476.584	845.177	7768.426	−17942.700	34009.420	−70098.100	138198.500
10	Curvilinear Trapezoidal	47.445	54.977	78.870	38.567	−104.356	66.681	26.862	−1.166
11	Exponential	80.030	104.400	117.172	137.448	111.043	108.105	84.930	49.374
12	F-	169.151	175.096	173.627	188.353	171.369	127.212	59.172	15.111
13	Gamma	70.579	74.097	−72.627	29.532	−136.866	95.561	54.305	20.160
14	Generalized Extreme Value	−43.159	48.494	−76.940	24.991	−171.255	84.548	20.200	−5.995
15	Generalized normal	−34.854	38.134	−79.260	27.950	−158.531	68.454	9.394	−17.742
16	Gumbel	43.451	68.983	−65.428	22.333	−163.084	115.082	71.632	36.051
17	Inverse Chi-Square	294.146	585.612	1643.540	−8710.210	15654.780	−33424.700	64926.670	−131900.000
18	Inverse Gamma	−9.974	50.348	−77.436	28.395	−151.218	94.513	41.369	9.622
19	Inverse Gaussian	6.488	50.197	−78.664	30.012	−143.270	91.323	42.122	8.749
20	Johnson SB	−32.829	−1.056	−80.267	30.228	−156.257	2.890	−45.077	−61.993
21	Johnson SU	−40.598	41.306	−76.737	−6.145	−239.022	118.059	31.683	−13.861
22	Laplace	25.287	72.537	−35.988	−6.437	−191.025	133.204	84.467	46.238
23	Logistic	55.755	86.843	−61.747	23.974	−148.058	120.729	90.417	61.297
24	Log-normal	−17.400	53.891	−77.864	29.698	−144.051	95.036	48.293	14.040
25	Normal	66.204	88.452	−65.597	30.007	−123.983	106.775	79.332	54.408
26	Rayleigh	56.486	74.218	46.217	77.131	22.894	72.398	54.576	33.811
27	Scaled/shifted t-	26.985	77.567	−67.602	−0.349	−191.455	139.852	100.640	63.352
28	Skewed-normal	54.281	47.797	−77.234	29.282	−151.624	83.945	28.828	1.019
29	Trapezoidal	74.027	65.204	−60.351	29.094	−127.149	66.087	12.789	−10.054
30	Triangular	72.673	45.922	−65.075	28.138	−129.258	62.014	9.177	−14.567
31	Uniform	281.826	559.045	1438.079	−10070.600	18327.550	−38661.500	75490.020	−152979.000
32	von Mises	66.102	90.813	−64.627	29.374	−127.377	111.819	86.116	60.624

Severe Drought (SD) for −1.50 to −1.99, and Extremely Dry or Drought (ED) is used for −2.00 and less.

4 | RESULTS

Figure 3 presents the temporal discrepancies between observed data and simulations (ACCESS-CM2, ACCESS-ESM1-5 and AWI-CM-1-1-MR). Similar behaviors were observed for the all the remaining models. In recent research, Yousaf et al. (2023) have also shown the temporal discrepancies among simulated data and model data at one random location in Tibet Plateau region. This proves the inherence of systematic errors (bias) with respect to observed data in all the GCMs. Parallel to historical period, the errors

TABLE 6 Selection of optimum model under BIC, AIC and AICs.

Model	Criterion	Base line		For MMQMSPI			For SPI		
		Observations	Ensemble	SSP1-2.6	SSP2-4.5	SSP5-8.5	SSP1-2.6	SSP2-4.5	SSP5-8.5
Gamma model	BIC	−364.472	−657.256	−155.417	−169.837	−130.771	71.92435	43.15542	22.6815
	AIC	70.56056	56.56814	−84.2567	20.10488	−138.667	63.71576	34.57599	14.01045
	AICc	70.57916	74.09699	72.6266	29.53196	−136.866	95.56105	54.30464	20.16037
Best univariate model	BIC	−441.157	−753.495	−267.339	−287.794	−240.328	−24.296	−30.8	−51.234
	AIC	−43.1958	−4.12958	−84.257	−16.638	−239.083	−37.977	−45.099	−65.685
	AICs	−43.1585	−1.05562	−80.2668	−10070.6	−17942.7	−38661.5	−70098.1	−152,979
K-CGMD	BIC	−2448.33	−5158.288	−2609.698	−2716.268	−2963.909	−1043.812	−1199.629	−1397.608
	AIC	293.5653	−629.1452	−366.6865	−1016.114	−1337.237	−1166.224	−1326.474	−1522.372
	AICs	294.0645	−628.646	−366.3803	−1015.807	−1336.93	−1165.917	−1326.167	−1522.065

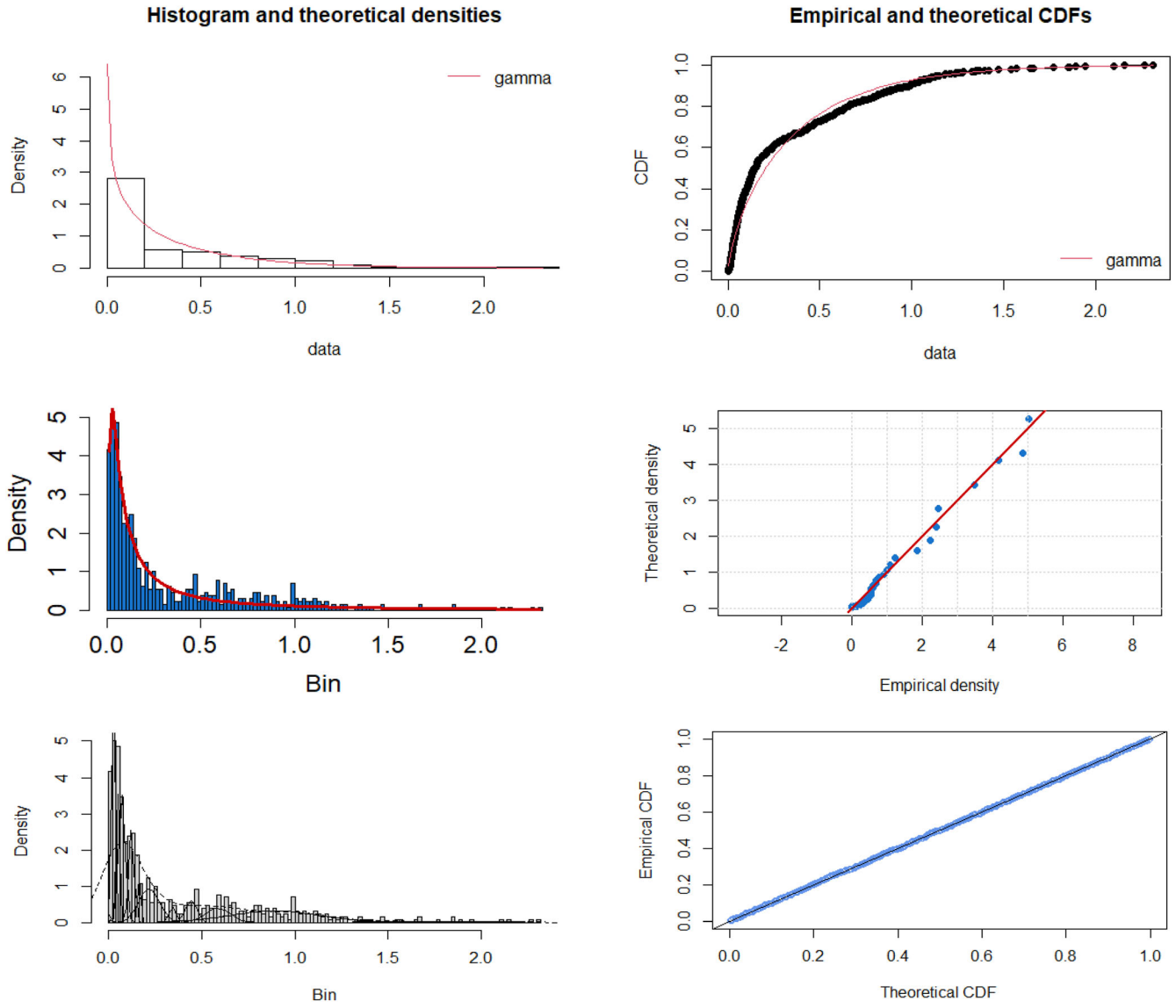

FIGURE 4 Optimal probability distributions for observed data: left to right and top to bottom: theoretical density and empirical and theoretical CDFs of Gamma distribution; theoretical density and empirical and theoretical CDFs of appropriate distribution; theoretical density, and empirical and theoretical CDFs of KCGMD. [Colour figure can be viewed at wileyonlinelibrary.com]

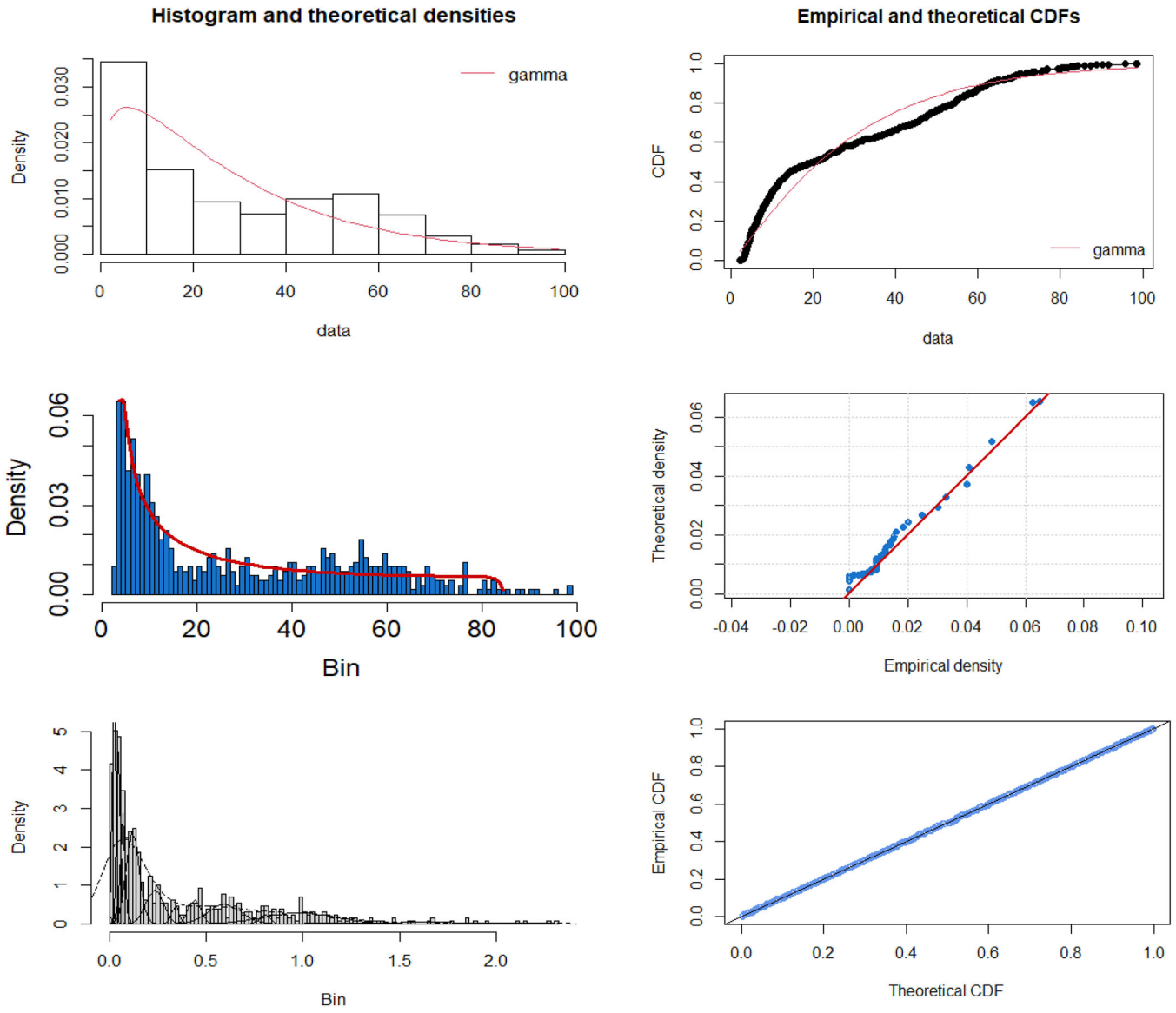

FIGURE 5 Optimal probability distributions for ensemble data: left to right and top to bottom: theoretical density and empirical and theoretical CDFs of Gamma distribution; theoretical density and empirical and theoretical CDFs of appropriate distribution; theoretical density, and empirical and theoretical CDFs of KCGMD. [Colour figure can be viewed at wileyonlinelibrary.com]

in future data of GCMs are evident. Therefore, removal of such bias is essential to increase the accuracy in multimodal ensemble.

Under the proposed framework, we used average time series for all the selected GCMs for bias correction of future data. To support the rational of the proposed framework, we tested the appropriateness of Gamma distribution as a bias correction model. Further, we employed varying distribution approach. Finally, we assessed the K-CGMM is more appropriate for removing bias in GCMs. The following subsections provide the detailed results and discussion on the findings of this research.

4.1 | Assessment of the appropriateness parametric models (Gamma, best univariate and K-CGMMD) for bias reduction

To assess the appropriateness of unimodal probability distribution, this research is based on 32 widely used univariate distributions. These are Generalized Extreme Value, Johnson SU, Generalized Normal, Johnson SB, Log-normal, Inverse Gamma, Inverse Gaussian, Cauchy, Laplace, Scaled/shifted t-, Gumbel, 3P Weibull, Curvilinear, Trapezoidal, 4P Beta, Logistic, Rayleigh, Skewed-normal, von Mises, Normal, Gamma, Triangular,

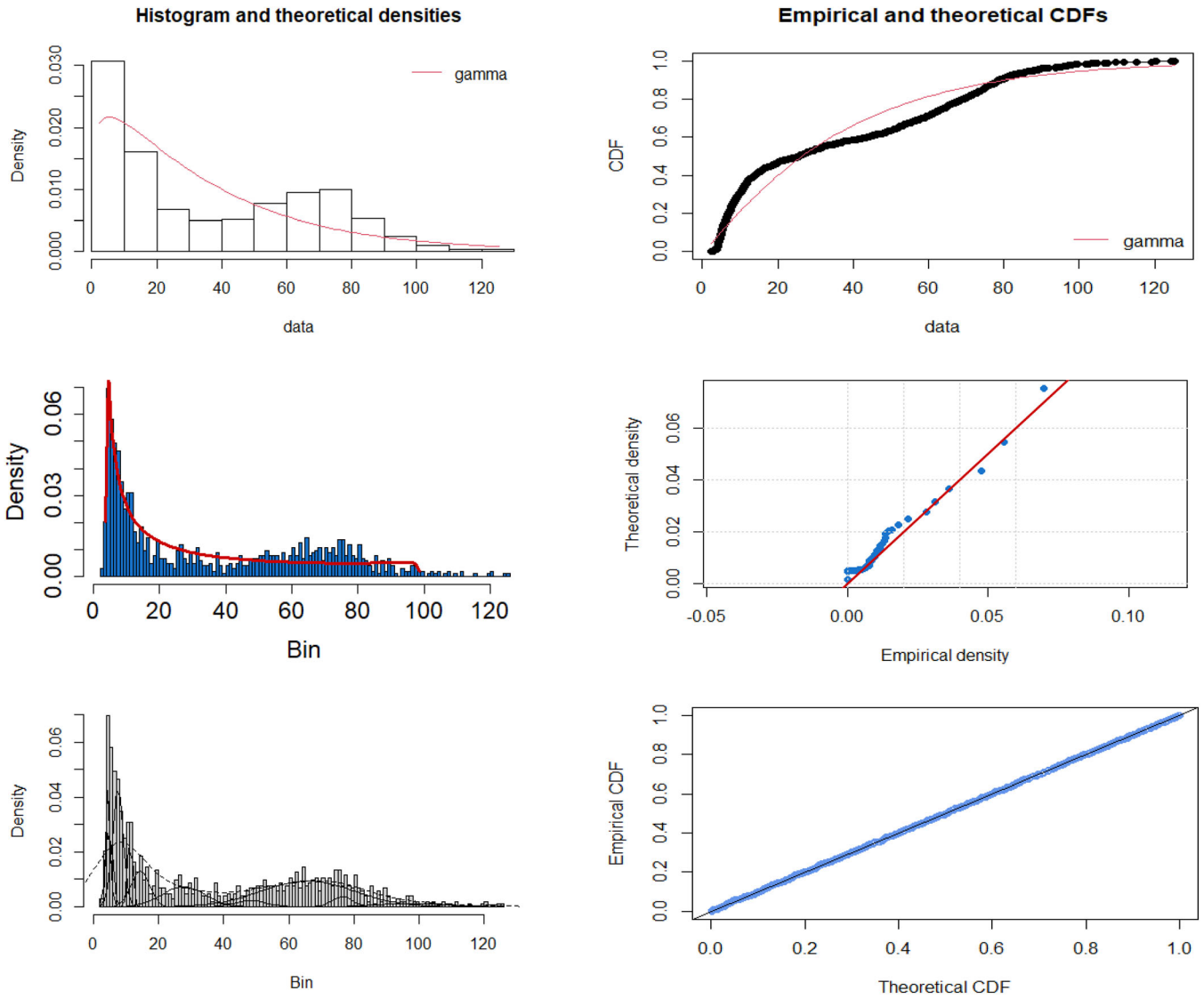

FIGURE 6 Optimal probability distributions for future scenario (SSP1-2.6): left to right and top to bottom: theoretical density and empirical and theoretical CDFs of Gamma distribution; theoretical density and empirical and theoretical CDFs of appropriate distribution; theoretical density, and empirical and theoretical CDFs of KCGMD. [Colour figure can be viewed at wileyonlinelibrary.com]

Exponential, Trapezoidal, 2P Beta, Chi, Chi-Square, F-, Arcsine, Cosine, Uniform, Inverse Chi-Square and Burr, were tested. Here, we used BIC, AIC and AICc as goodness-of-fit criteria to assess the most appropriate probability model. However, our decision regarding model selection mainly relies on BIC due to its consistent properties.

To verify it BIC values for the observed, the ensemble and three different future scenario data sets have been calculated. Tables 3–6 show the BIC, AIC and AICc values of all the 32 univariate distributions (presented in ascending order), including the gamma distribution. We observed that the Johnson Sb has the lowest BIC among all distributions. Figure 4 shows the graphical assessment of gamma, best univariate model, and K-CGMMD on the observed data. Similarly, the probability behavior of ensemble data in reference period and future scenarios (SSP1-2.6, SSP1-4.5 and SSP1-8.5) are presented in Figures 4–8, respectively. From these figures, we assessed that the K-CHMD is best model with lowest uncertainty. Further, the lowest values of BICs in K-CGMD also support its optimality (see Table 4).

Table 7 shows the means and variance of twelve of K-CGMD. On the same lines, the appropriateness of K-CGMD was assessed and found its superiority over the univariate probability models including gamma distributions in all the grids points. After assessing the superiority, we performed the bias

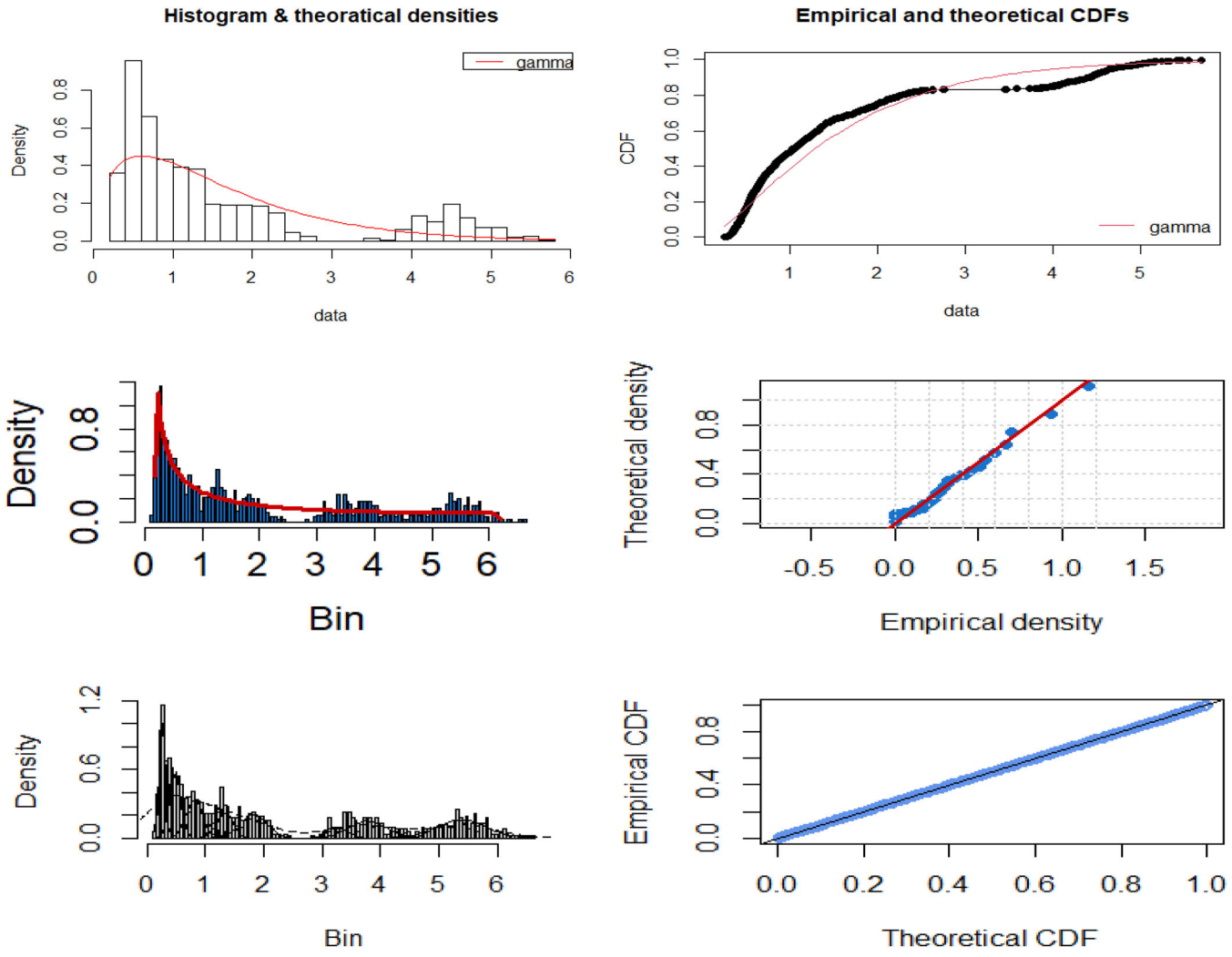

FIGURE 7 Optimal probability distributions for future scenario (SSP1-4.5): left to right and top to bottom: theoretical density and empirical and theoretical CDFs of Gamma distribution; theoretical density and empirical and theoretical CDFs of appropriate distribution; theoretical density, and empirical and theoretical CDFs of KCGMD. [Colour figure can be viewed at wileyonlinelibrary.com]

correction procedure to the future data of all scenarios under the K-CGMD.

4.2 | Computation of MMQMSPI

After correcting the bias, we standardized the ensemble data for future scenarios to obtain the drought indices. Before computing the MMQMSPI for all time scales, we assessed the deviation between the proposed ensemble and SAS across all future scenarios at the one-month time scale. Figure 9 displays the violin plots of the ensemble data under both schemes and the temporal plot of MMQMSPI and SPI at the 1-month time scale. We inferred that both the ensemble and temporal data differed, demonstrating the effectiveness of the proposed scheme in obtaining standardized indices. Figures 10–12 show the temporal behavior of MMQMSPI at various time scales under SSP1-2.6, SSP2-4.5 and SSP5-8.5, respectively. From these figures, we observed that the most parts of the Tibetan Plateau experienced severe drought from 2020 to 2023. This period was characterized by significantly reduced precipitation levels and prolonged dry conditions across the region. These drought impacts have been documented through various meteorological observations and studies focusing on water availability and ecological changes in the Tibetan Plateau during those years (Lin et al., 2023; Liu et al., 2020; Shao et al., 2023). In the next stage, the K-CGMD was accurately implemented into the recommended procedure of bias correction. Further, bias corrected data was used into three different scenarios, that is, scenario-1 (SSP1-2.6), scenario-2 (SSP2-4.5) and scenario-3

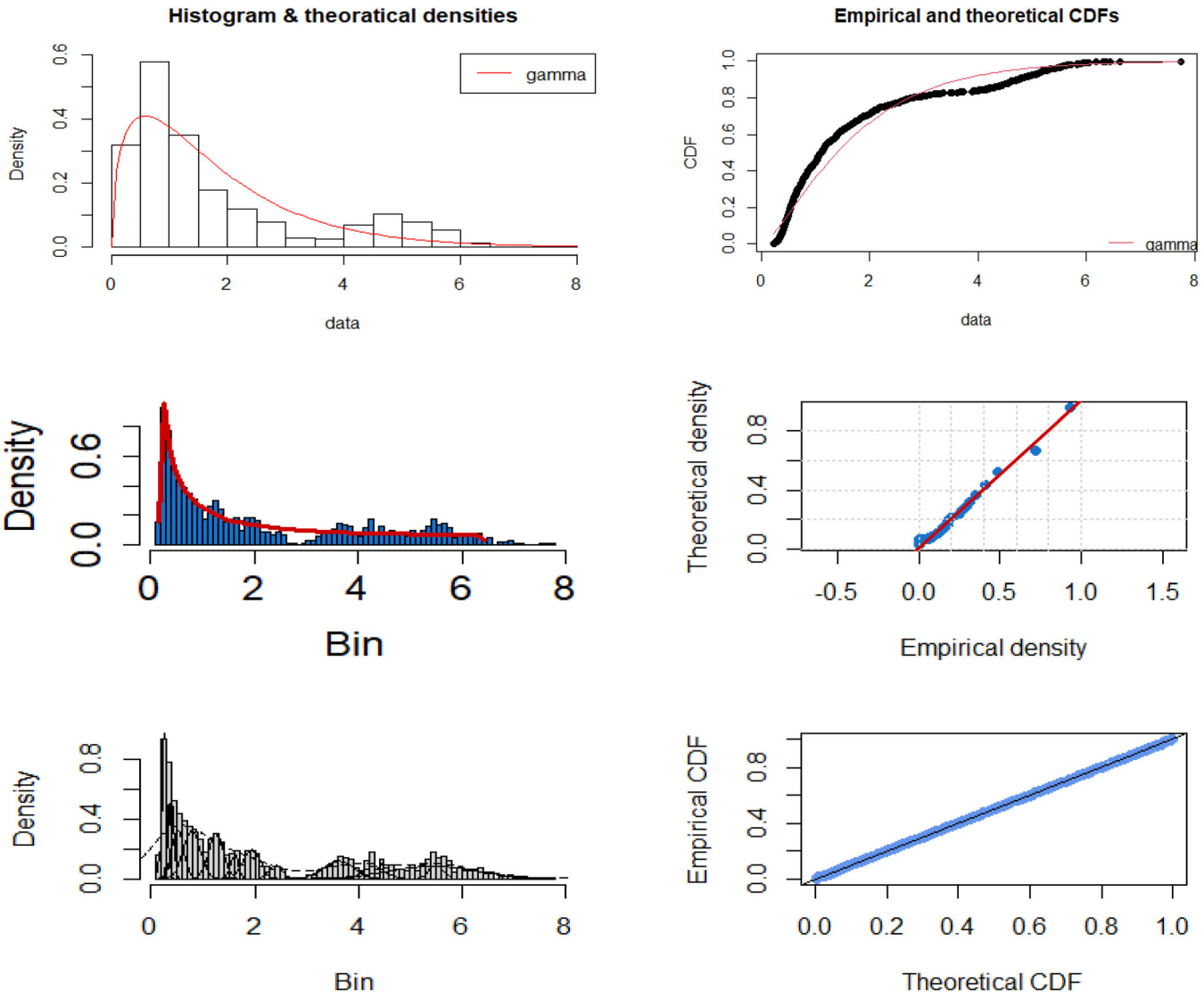

FIGURE 8 Optimal probability distributions for future scenario (SSP1-8.5): left to right and top to bottom: theoretical density and empirical and theoretical CDFs of Gamma distribution; theoretical density and empirical and theoretical CDFs of appropriate distribution; theoretical density, and empirical and theoretical CDFs of KCGMD. [Colour figure can be viewed at wileyonlinelibrary.com]

(SSP5-8.5) to better forecast the future for (2015–2100). For the analysis purpose seven different time scales of the precipitation data has been used, that is, 1–3–6–9–12–24–48 months. The nonparametric approach was applied to standardize the data and proposed a new drought index named as Multi-Model Quantile Mapped Standardized Precipitation Index (MMQMSPI). Initially, the optimal probability distributions were assessed by observed data in Figure 4, for ensemble data in Figure 5, for SSP1-2.6 in Figure 6, for SSP1-4.5 in Figure 7 and for SSP1-8.5 in Figure 8.

The correct distribution of all data sets was evaluated before applying QM. In this regard, three distributions were considered, that is, Gamma, best fitted uni-variate distribution out of 32 distributions and KCGMD. Histogram and theoretical densities, empirical and theoretical CDFs, based on the gamma distribution are shown in the first row and the data does not appear to be nearly a straight line, and we assessed that the gamma was not the best fit distribution for those data sets. Histogram and theoretical densities were also not in favor of applying gamma as a fitted distribution. However, there were significant discrepancies between the two curves, empirical and theoretical curves, which indicate that the observed, ensemble and scenario data did not fit the chosen theoretical distribution well. The un-variate distribution displayed the density graph of the Johnson SB distribution as the best fitted univariate distribution among 32 selected distributions for the observed ensemble

and all three scenario data sets shown in the second row. The K-component Gaussian mixture density plot with 12 components was also plotted and supported it best over uni-variate based on their empirical and theoretical CDFs.

The suggested drought index (MMQMSPI) for scenario-1 (SSP1-2.6) is presented on seven different time scales in Figure 8.

Temporal behavior clearly shows the monthly variation in the pattern of MMQMSPI and these variations are different on each time scale. Red and blue colors represent the dry and the wet probabilities respectively. Index-1 shows a 1-month time scale, index-3 represents 3 months' time scale and so on, index-48 represents the time scale of 48 months. The probabilities under SSP1-2.6 at different times suggest that the likelihood of wet conditions is higher than that of dry ones and is fluctuating at different time scales.

Figures 11 and 12 display the temporal behavior of MMQMSPI by using scenario-2 (SSP2-4.5) and scenario-3 (SSP5-8.5) and provide scales of dry and wet conditions based on probabilities at various time scales for one grid point. It is also implied by the probabilities under SSP2-4.5 and SSP5-8.5 at various time periods that there is a lower chance of dry circumstances than wet ones. These findings suggest a drastic change over the long term; drought conditions after 2050. Extreme dry and wet conditions, with a higher probability can be seen clearly in both scenarios. Building sustainable and resilient societies may be helped by using these findings to guide efforts in risk assessment, land use planning, and water resource management. Consequently, quick action is essential to mitigate the adverse consequences of the drought in the TP.

5 | DISCUSSION

The main objective of the study was to introduce a new and better framework of bias correction and improve the accuracy of drought monitoring. In the past, the majority of researchers suggested gamma as the best fitted distribution in their studies. Some others use different uni-variable distributions while dealing with precipitation data. But not all the data sets follow one peak distribution and can contain multiple peaks. So, here in this paper we used and compared precipitation data of 18 GCMs on 32 randomly selected locations in TP by applying a mixture of distributions. In the early stages of research, the plots helped to verify the best fitted distribution between 32 univariate distributions and compared them with KCGMD. Further, BIC indicated that KCGMD is the best fitted distribution. So, we corrected precipitation data by applying KCGMD with twelve components, including a quantile mapping technique. Three types of data sets were incorporated through a simple average scheme on two past data sets (1960–2014), and one for future scenario data (2015–2100). The past data includes observed and ensemble data. On the other hand, future data was based on three different scenarios used one at a time. In this manner, three settings were used to find bias-corrected data. The first setting was based on scenario-1

TABLE 7 Components wise distribution of mean and variances under K-CGM model.

	Observation		Ensemble		SSP1-2.6		SSP2-4.5		SSP5-8.5	
Components	**Mean**	**Variance**	**Mean**	**Variance**	**Mean**	**Variance**	**Mean**	**Variance**	**Mean**	**Variance**
1	0.1870	0.0726	0.2068	0.0277	0.2378	0.0126	0.2505	0.0489	0.1805	0.0141
2	0.5165	0.1914	0.2575	0.0066	0.2826	0.0569	0.2819	0.0008	0.2550	0.0247
3	1.0670	0.1276	0.3433	0.0509	0.4143	0.0150	0.3621	0.0147	0.3718	0.0687
4	4.7455	1.2865	0.3708	0.0119	0.4864	0.1118	0.4796	0.1012	0.6769	0.1845
5	1.2195	0.0010	0.9586	0.0259	0.7990	0.1033	1.5907	0.0045	1.2452	0.1701
6	1.5630	0.1550	0.7271	0.0841	2.6272	0.0326	0.8015	0.1275	1.6171	0.0628
7	2.3755	0.6626	1.1597	0.2064	1.7967	0.1910	1.2617	0.1546	1.9416	0.1590
8	7.6805	0.6946	1.8085	0.0079	1.3051	0.2020	1.8358	0.2340	2.4118	0.1314
9	9.0531	0.3888	1.6241	0.0999	3.2690	0.1739	5.2858	0.5338	3.6201	0.2819
10	5.1323	0.1342	2.0443	0.3038	3.7201	0.2971	3.6383	0.3658	4.3140	0.2059
11	6.5013	0.0553	2.9364	0.1553	5.4175	0.2996	5.4264	0.1720	5.5078	0.1291
12	10.2111	0.9099	3.2894	0.2115	5.5177	0.4733	5.7997	0.0413	5.4508	0.8341

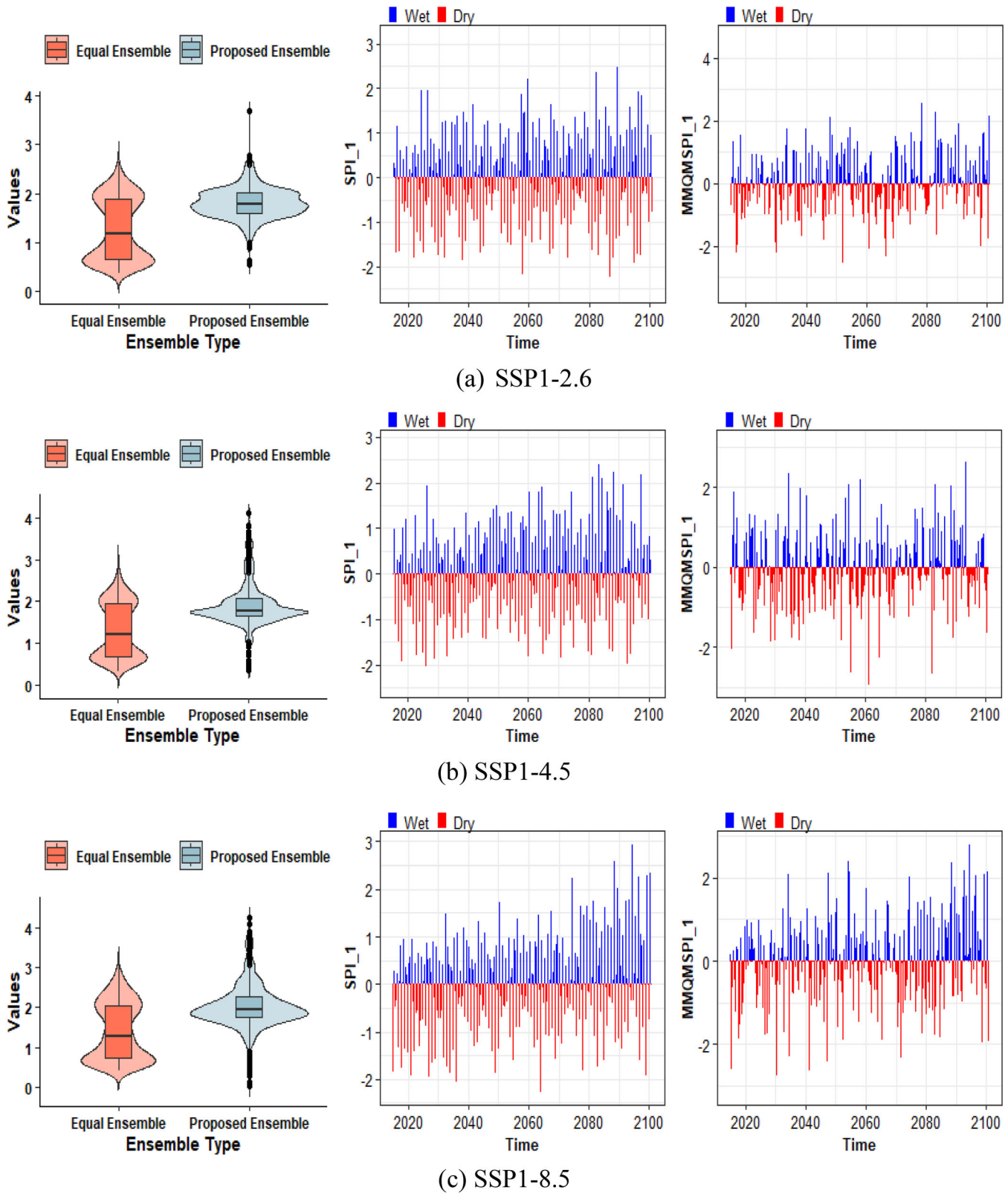

FIGURE 9 Violin plot and temporal plots based on proposed ensemble data and equal ensemble scheme (SAS) under various scenarios. [Colour figure can be viewed at wileyonlinelibrary.com]

(SSP1-2.6), second on scenario-2 (SSP2-4.5) and third on scenario-3 (SSP5-8.5). Three further scenarios were used to predict the future and a nonparametric approach was used on bias-corrected data to standardize it. A new drought index was also proposed and future patterns of weather were deducted. Seven different time

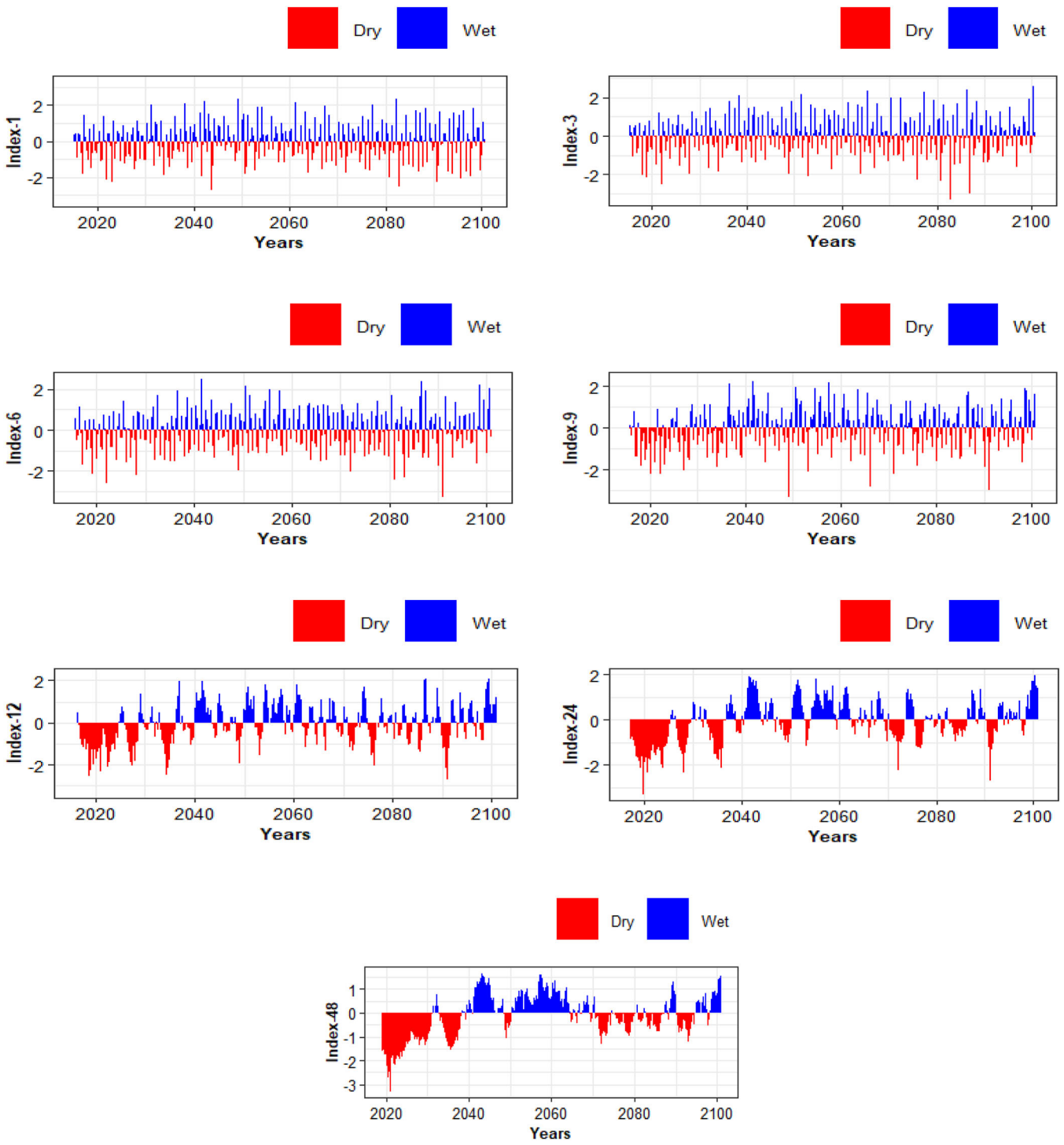

FIGURE 10 Temporal behavior of MMQMSPI in various time scales under SSP1-2.6. [Colour figure can be viewed at wileyonlinelibrary.com]

scales were used for the purpose of forecasting. From the results of this research, we inferred that the probability of experiencing wet conditions is greater than those of dry conditions, and these probabilities vary over different time scales. Under, SPI drought index, these results are consistent with the finding presented Li et al. (2022). On the other hand, the findings of this research present a different perspective compared to those of Yang et al. (2015). Yang et al. (2015) projected future drought in TB using the SPI drought index. In contrast, Sun et al. (2019) demonstrated that under both RCP 4.5 and RCP 8.5 scenarios, drought conditions are expected to occur at certain stations based on the SPI index. The differing inferences regarding drought may

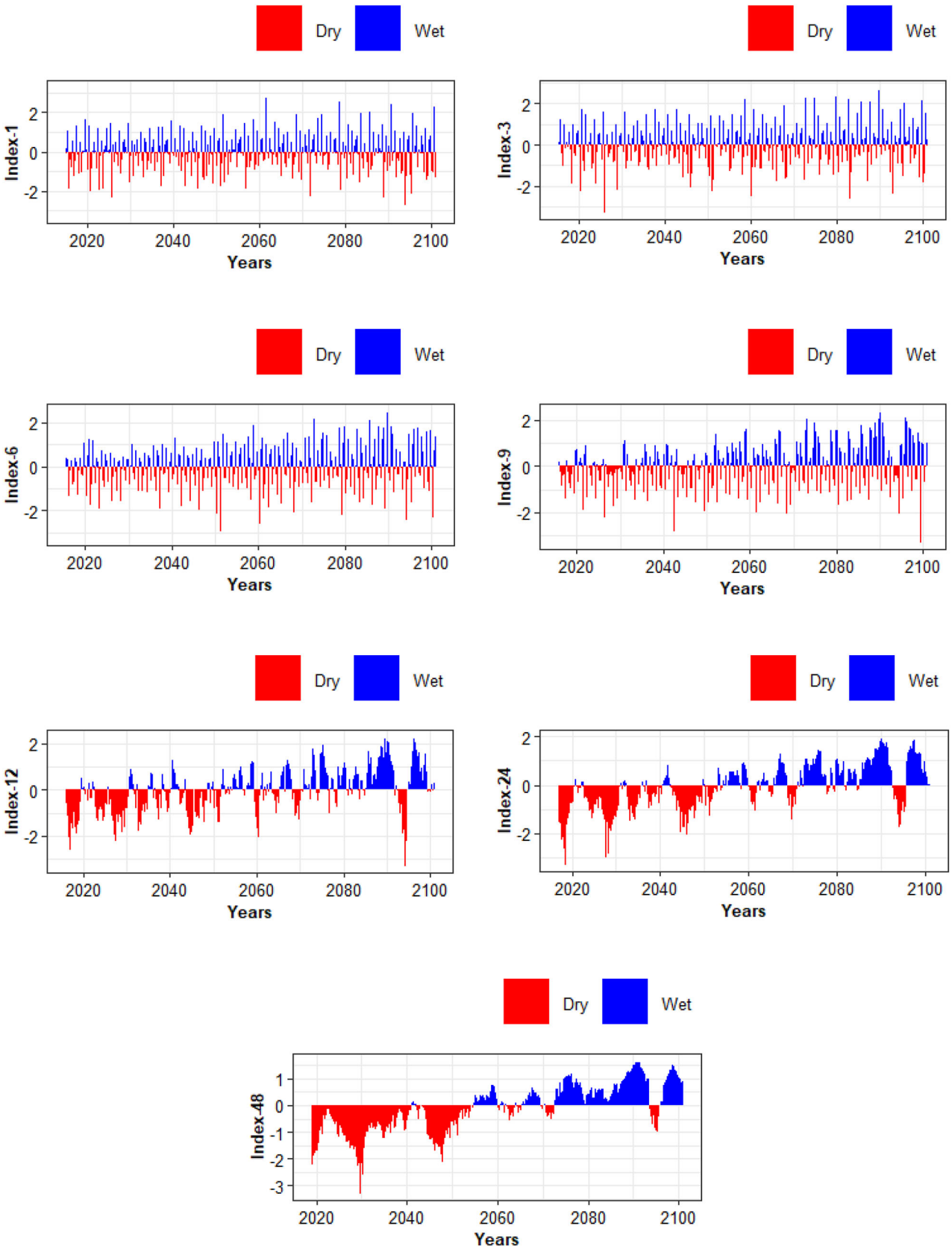

FIGURE 11 Temporal behavior of MMQMSPI in various time scales under SSP2-4.5. [Colour figure can be viewed at wileyonlinelibrary.com]

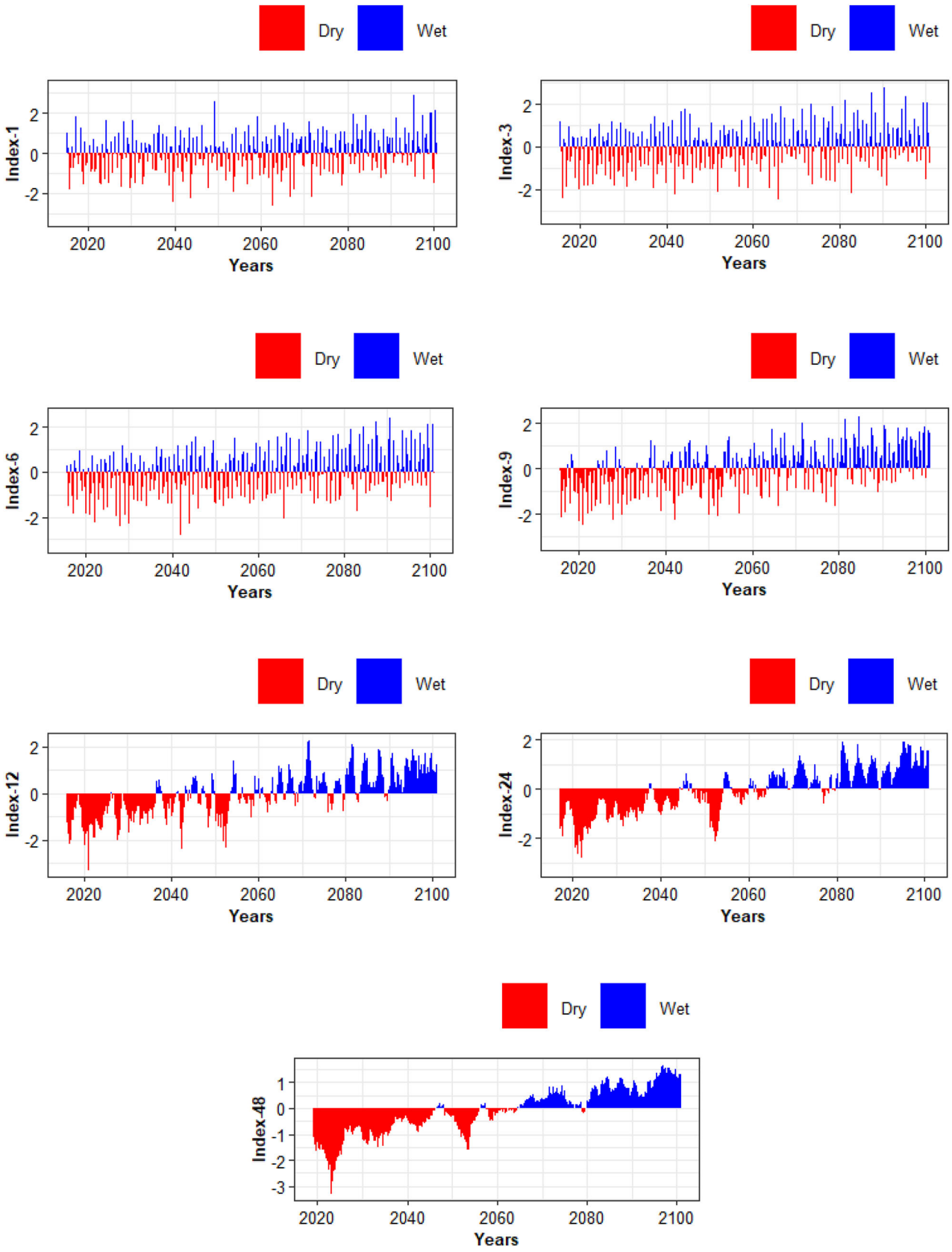

FIGURE 12 Temporal behavior of MMQMSPI in various time scales under SSP5-8.5. [Colour figure can be viewed at wileyonlinelibrary.com]

be due to variations in the estimation procedures or the use of different simulations.

6 | CONCLUSION

The role of GCM simulations in integrating drought indices is paramount in drought monitoring systems. However, biases (systematic errors) in GCM data and uncertainties in standardization approaches reduce the scope for accurately assessing future drought. This study introduces a new statistical framework for the accurate assessment of drought in the 21st century under multiple GCM simulations. The proposed framework consists of (1) a bias correction procedure, and (2) optimal standardization. In the bias correction procedure, we introduce the K-CGMD based inference quantile method. For optimal standardization, we use the best model, whether probabilistic or nonparametric. In this application, 32 randomly scattered grid points around the Tibetan Plateau region are considered. Gridded interpolated data from the CN0.5 model are used as observations, while simulated data from 18 GCMs of CMIP6 are considered. The findings related to the ensemble of GCMs clearly indicate that K-CGMD is more appropriate than univariate models. Furthermore, this study finds that generally, a single model is not appropriate for standardization. Taken together, these findings suggest the vital role of advanced probability models in improving ensembles and standardization. This study establishes a quantitative framework for the accurate assessment of drought under multiple GCM models. It is the first study to present evidence of using Gaussian mixture probability models for bias correction. Although this study is based on a small number of grid points, the findings suggest that improved spatiotemporal analysis of drought can be achieved by increasing the number of grid points accordingly. However, these findings are limited by the use of precipitation data only. Further studies need to be carried out to include more climatic parameters such as temperature, solar radiation and wind speed.

AUTHOR CONTRIBUTIONS

Rubina Naz: Conceptualization; methodology; software; formal analysis; writing – original draft. **Zulfiqar Ali:** Conceptualization; supervision; data curation; writing – review and editing; visualization. **Veysi Kartal:** Writing – review and editing. **Mohammed A. Alshahrani:** Validation. **Shreefa O. Hilali:** Software. **Fathia Moh. Al Samman:** Resources.

ACKNOWLEDGMENT

The authors extend their appreciation to the Deanship of Research and Graduate Studies at King Khalid University for funding this work through Large Research Project under grant number RGP. 2/115/45", the authors also express their appreciation to the Deanship of Scientific Research at Northern Border University, Arar, Saudi Arabia for funding this research work through project number "NBU-FFR-2024-1324-04". And this study is supported via funding from Prince Sattam bin Abdulaziz University project number (PSAU/2024/R/1445).

CONFLICT OF INTEREST STATEMENT

The authors declare no conflicts of interest.

DATA AVAILABILITY STATEMENT

The data that support the findings of this study are available from the corresponding author upon reasonable request.

REFERENCES

Abramowitz, M. & Stegun, I.A. (1968) *Handbook of mathematical functions with formulas, graphs, and mathematical tables*, Vol. 55. Dover, NY: US Government Printing Office.

Adeyeri, O.E., Zhou, W., Laux, P., Ndehedehe, C.E., Wang, X., Usman, M. et al. (2023) Multivariate drought monitoring, propagation, and projection using bias-corrected general circulation models. *Earth's Futures*, 11(4), e2022EF003303.

Ahmad, M., Ali, Z., Ilyas, M., Mohsin, M. & Niaz, R. (2023) A common factor analysis based data mining procedure for effective assessment of 21st century drought under multiple global climate models. *Water Resources Management*, 37(12), 4787–4806.

Ali, F., Li, B.Z. & Ali, Z. (2021) Strengthening drought monitoring module by ensembling auxiliary information based varying estimators. *Water Resources Management*, 35(10), 3235–3252.

Ali, Z., Hussain, I., Faisal, M., Grzegorczyk, M., Qamar, S., Shoukry, A.M. et al. (2020a) On the more generalized nonparametric framework for the propagation of uncertainty in drought monitoring. *Meteorological Applications*, 27(3), e1914.

Ali, Z., Hussain, I., Faisal, M., Nazir, H.M., Moemen, M.A.E., Hussain, T. et al. (2017) A novel multi-scalar drought index for monitoring drought: the standardized precipitation temperature index. *Water Resources Management*, 31, 4957–4969.

Ali, Z., Hussain, I., Grzegorczyk, M.A., Ni, G., Faisal, M., Qamar, S. et al. (2020b) Bayesian network based procedure for regional drought monitoring: the seasonally combinative regional drought indicator. *Journal of Environmental Management*, 276, 111296.

Ali, Z., Qamar, S., Khan, N., Faisal, M. & Sammen, S. S. (2023) A new regional drought index under X-bar chart based weighting scheme–The quality boosted regional drought index (QBRDI). *Water Resources Management*, 37(5), 1895–1911.

An, P., Wang, Z. & Zhang, C. (2022) Ensemble unsupervised autoencoders and Gaussian mixture model for cyberattack detection. *Information Processing & Management*, 59(2), 102844.

Anghel, C.G. & Ilinca, C. (2022) Parameter estimation for some probability distributions used in hydrology. *Applied Sciences*, 12(24), 12588.

Banholzer, S., Kossin, J. & Donner, S. (2014) The impact of climate change on natural disasters. In: *Reducing disaster: Early*

warning systems for climate change. Dordrecht, The Netherlands: Springer, pp. 21–49.

Basak, D., Nagababu, G., Puppala, H., Patel, J. & Kumar, S.V.A. (2023) Foreseeing the spatio-temporal offshore wind energy potential of India using a differential weighted ensemble created using CMIP6 datasets. *Regional Studies in Marine Science*, 65, 103066.

Batool, A., Ali, Z., Mohsin, M. & Shakeel, M. (2023) A generalized procedure for joint monitoring and probabilistic quantification of extreme climate events at regional level. *Environmental Monitoring and Assessment*, 195(10), 1223.

Benaglia, T., Chauveau, D., Hunter, D.R. & Young, D.S. (2010) mixtools: an R package for analyzing mixture models. *Journal of Statistical Software*, 32, 1–29.

Chen, K., Wang, B., Chen, C. & Zhou, G. (2022) MaxEnt modeling to predict the current and future distribution of Pomatosace filicula under climate change scenarios on the Qinghai–Tibet plateau. *Plants*, 11(5), 670.

Conover, W.J. & Iman, R.L. (1981) Rank transformations as a bridge between parametric and nonparametric statistics. *American Statistician*, 35(3), 124–129.

Conover, W.J. (2012) The rank transformation—an easy and intuitive way to connect many nonparametric methods to their parametric counterparts for seamless teaching introductory statistics courses. *Wiley Interdisciplinary Reviews: Computational Statistics*, 4(5), 432–438.

Cook, B.I., Mankin, J.S. & Anchukaitis, K.J. (2018) Climate change and drought: From past to future. *Current Climate Change Reports*, 4, 164–179.

Danandeh Mehr, A., Sorman, A.U., Kahya, E. & Hesami Afshar, M. (2020) Climate change impacts on meteorological drought using SPI and SPEI: case study of Ankara, Turkey. *Hydrological Sciences Journal*, 65(2), 254–268.

Dong, F., Javed, A., Saber, A., Neumann, A., Arnillas, C.A., Kaltenecker, G. et al. (2021) A flow-weighted ensemble strategy to assess the impacts of climate change on watershed hydrology. *Journal of Hydrology*, 594, 125898.

Enayati, M., Bozorg-Haddad, O., Bazrafshan, J., Hejabi, S. & Chu, X. (2021) Bias correction capabilities of quantile mapping methods for rainfall and temperature variables. *Journal of Water and Climate Change*, 12(2), 401–419.

Erhardt, T.M. & Czado, C. (2018) Standardized drought indices: a novel univariate and multivariate approach. *Journal of the Royal Statistical Society Series C: Applied Statistics*, 67(3), 643–664.

Fan, M., Lu, D., Rastogi, D. & Pierce, E.M. (2022) A spatiotemporal-aware weighting scheme for improving climate model ensemble predictions. *Journal of Machine Learning for Modeling and Computing*, 3(4), 29–55.

Farahmand, A. & AghaKouchak, A. (2015) A generalized framework for deriving nonparametric standardized drought indicators. *Advances in Water Resources*, 76, 140–145.

Fesl, B., Turan, N., Joham, M. & Utschick, W. (2023) Learning a Gaussian mixture model from imperfect training data for robust channel estimation. *IEEE Wireless Communications Letters*, 12(6), 1066–1070.

Gaur, S., Singh, R., Bandyopadhyay, A. & Singh, R. (2023) Diagnosis of GCM-RCM-driven rainfall patterns under changing climate through the robust selection of multi-model ensemble and sub-ensembles. *Climatic Change*, 176(2), 13.

Gholami, H., Lotfirad, M., Ashrafi, S.M., Biazar, S.M. & Singh, V.P. (2023) Multi-GCM ensemble model for reduction of uncertainty in runoff projections. *Stochastic Environmental Research and Risk Assessment*, 37(3), 953–964.

Gutiérrez, J.M., Jones, R.G. & Narisma, G.T. (2021) IPCC interactive Atlas. In: *Climate change 2021: the physical science basis. contribution of working group I to the sixth assessment report of the intergovernmental panel on climate change*. Cambridge: Cambridge University Press.

Hagemann, S., Chen, C., Haerter, J.O., Heinke, J., Gerten, D. & Piani, C. (2011) Impact of a statistical bias correction on the projected hydrological changes obtained from three GCMs and two hydrology models. *Journal of Hydrometeorology*, 12(4), 556–578.

Hao, Z., Hao, F., Singh, V.P. & Zhang, X. (2018) Quantifying the relationship between compound dry and hot events and El Niño–Southern Oscillation (ENSO) at the global scale. *Journal of Hydrology*, 567, 332–338.

Hausfather, Z., Drake, H.F., Abbott, T. & Schmidt, G.A. (2020) Evaluating the performance of past climate model projections. *Geophysical Research Letters*, 47(1), e2019GL085378.

Heo, J.H., Ahn, H., Shin, J.Y., Kjeldsen, T.R. & Jeong, C. (2019) Probability distributions for a quantile mapping technique for a bias correction of precipitation data: a case study to precipitation data under climate change. *Water*, 11(7), 1475.

Hipel, K.W. & Fang, L. (2013) *Stochastic and statistical methods in hydrology and environmental engineering: Effective environmental management for sustainable development*, Vol. 4. Southampton, UK: WIT Press.

Hoylman, Z.H., Bocinsky, R.K. & Jencso, K.G. (2022) Drought assessment has been outpaced by climate change: empirical arguments for a paradigm shift. *Nature Communications*, 13(1), 2715.

Huang, Y., Xin, Z., Dor-ji, T. & Wang, Y. (2022) Tibetan Plateau greening driven by warming-wetting climate change and ecological restoration in the 21st century. *Land Degradation & Development*, 33(14), 2407–2422.

Huang, Z., Zhao, T., Zhang, Y., Cai, H., Hou, A. & Chen, X. (2021) A five-parameter Gamma-Gaussian model to calibrate monthly and seasonal GCM precipitation forecasts. *Journal of Hydrology*, 603, 126893.

Jehanzaib, M., Sattar, M.N., Lee, J.H. & Kim, T.W. (2020) Investigating effect of climate change on drought propagation from meteorological to hydrological drought using multi-model ensemble projections. *Stochastic Environmental Research and Risk Assessment*, 34, 7–21.

Jiang, C., Xiong, L. & Xu, W. (2023) Nonstationary hydrological distribution estimation using hierarchical model with stochastic covariates. *Journal of Hydrologic Engineering*, 28(4), 04023009.

Kassim, M. (2020) Current and future intensity-duration-frequency curves based on weighted ensemble GCMs and temporal disaggregation. *Sains Malaysiana*, 49(10), 2359–2371.

Katsevich, A. & Bandeira, A.S. (2023) Likelihood maximization and moment matching in low SNR Gaussian mixture models. *Communications on Pure and Applied Mathematics*, 76(4), 788–842.

Khan, J.U., Islam, A.S., Das, M.K., Mohammed, K., Bala, S.K. & Islam, G.T. (2020) Future changes in meteorological drought characteristics over Bangladesh projected by the CMIP5 multi-model ensemble. *Climatic Change*, 162, 667–685.

Kheir, A.M., Elnashar, A., Mosad, A. & Govind, A. (2023) An improved deep learning procedure for statistical downscaling of climate data. *Heliyon*, 9(7), e18200.

Lalande, M., Ménégoz, M., Krinner, G., Ottlé, C. & Cheruy, F. (2023) Reducing the High Mountain Asia cold bias in GCMs by adaptingsnow cover parameterization to complex topography areas. *Cryosphere Discussions*, 2023, 1–54.

Leys, C. & Schumann, S. (2010) A nonparametric method to analyze interactions: the adjusted rank transform test. *Journal of Experimental Social Psychology*, 46(4), 684–688.

Li, X., Zhang, K., Gu, P., Feng, H., Yin, Y., Chen, W. et al. (2021) Changes in precipitation extremes in the Yangtze River Basin during 1960–2019 and the association with global warming, ENSO, and local effects. *Science of the Total Environment*, 760, 144244.

Li, Z., Ali, Z., Cui, T., Qamar, S., Ismail, M., Nazeer, A. et al. (2022) A comparative analysis of pre-and post-industrial spatiotemporal drought trends and patterns of Tibet Plateau using Sen slope estimator and steady-state probabilities of Markov Chain. *Natural Hazards*, 113(1), 547–576.

Lin, H., Yu, Z., Chen, X., Gu, H., Ju, Q. & Shen, T. (2023) Spatial-temporal dynamics of meteorological and soil moisture drought on the Tibetan Plateau: trend, response, and propagation process. *Journal of Hydrology*, 626, 130211.

Liu, Y., Li, Y., Huang, J., Zhu, Q. & Wang, S. (2020) Attribution of the Tibetan Plateau to northern drought. *National Science Review*, 7(3), 489–492.

Ma, Q., Li, X., Wu, S. & Zeng, F. (2022) Potential geographical distribution of Stipa purpurea across the Tibetan Plateau in China under climate change in the 21st century. *Global Ecology and Conservation*, 35, e02064.

Manoukian, E.B. (2022) *Mathematical nonparametric statistics*. New York: Gordan & Breach Science Publishers.

Masson-Delmotte, V., Zhai, P., Pörtner, H.O., Roberts, D., Skea, J. & Shukla, P.R. (2022) *Global Warming of 1.5°C: IPCC special report on impacts of global warming of 1.5°C above pre-industrial levels in context of strengthening response to climate change, sustainable development, and efforts to eradicate poverty*. Cambridge: Cambridge University Press.

McKee, T.B., Doesken, N.J. & Kleist, J. (1993) The relationship of drought frequency and duration to time scales. In: *Proceedings of the 8th conference on applied climatology*. Anaheim, CA: American Meteorological Society, pp. 179–183.

Nahar, J., Johnson, F. & Sharma, A. (2017) Assessing the extent of non-stationary biases in GCMs. *Journal of Hydrology*, 549, 148–162.

Naz, R. & Ali, Z. (2024) A novel self-adjusting weight approximation procedure to minimize non-identical seasonal effects in multimodel ensemble for accurate twenty-first century drought assessment. *Stochastic Environmental Research and Risk Assessment*, 38, 2451–2472.

Niranjan Kumar, K., Thota, M.S., Ashrit, R., Mitra, A.K. & Rajeevan, M.N. (2022) Quantile mapping bias correction methods to IMDAA reanalysis for calibrating NCMRWF unified model operational forecasts. *Hydrological Sciences Journal*, 67(6), 870–885.

Ohn, I. & Lin, L. (2023) Optimal Bayesian estimation of Gaussian mixtures with growing number of components. *Bernoulli*, 29(2), 1195–1218.

Pagowski, M., Grell, G.A., McKeen, S.A., Dévényi, D., Wilczak, J.M., Bouchet, V. et al. (2005) A simple method to improve ensemble-based ozone forecasts. *Geophysical Research Letters*, 32(7), L07814.

Pastén-Zapata, E., Jones, J.M., Moggridge, H. & Widmann, M. (2020) Evaluation of the performance of Euro-CORDEX Regional Climate Models for assessing hydrological climate change impacts in Great Britain: a comparison of different spatial resolutions and quantile mapping bias correction methods. *Journal of Hydrology*, 584, 124653.

Peng, S., Wang, C., Li, Z., Mihara, K., Kuramochi, K., Toma, Y. et al. (2023) Climate change multi-model projections in CMIP6 scenarios in Central Hokkaido, Japan. *Scientific Reports*, 13(1), 230.

Rajulapati, C.R. & Papalexiou, S.M. (2023) Precipitation bias correction: a novel semi-parametric quantile mapping method. *Earth and Space Science*, 10(4), e2023EA002823.

Schwarz, G. (1978) Estimating the dimension of a model. *Annals of Statistics*, 6, 461–464.

Seo, G.Y. & Ahn, J.B. (2023) Comparison of bias correction methods for summertime daily rainfall in South Korea using quantile mapping and machine learning model. *Atmosphere*, 14(7), 1057.

Shao, X., Zhang, Y., Ma, N., Zhang, X., Tian, J. & Liu, C. (2023) Flood increase and drought mitigation under a warming climate in the Southern Tibetan Plateau. *Journal of Geophysical Research: Atmospheres*, 128(2), e2022JD037835.

Shiau, J.T. (2020) Effects of gamma-distribution variations on SPI-based stationary and nonstationary drought analyses. *Water Resources Management*, 34, 2081–2095.

Shin, J.Y., Lee, T., Park, T. & Kim, S. (2019) Bias correction of RCM outputs using mixture distributions under multiple extreme weather influences. *Theoretical and Applied Climatology*, 137, 201–216.

Shirmohammadi, B., Rostami, M., Varamesh, S., Jaafari, A. & Taie Semiromi, M. (2024) Future climate-driven drought events across Lake Urmia, Iran. *Environmental Monitoring and Assessment*, 196(1), 24.

Song, Y.H., Chung, E.S. & Shahid, S. (2022) The new bias correction method for daily extremes precipitation over South Korea using CMIP6 GCMs. *Water Resources Management*, 36(15), 5977–5997.

Song, Z., Xia, J., She, D., Li, L., Hu, C. & Hong, S. (2021) Assessment of meteorological drought change in the 21st century based on CMIP6 multi-model ensemble projections over mainland China. *Journal of Hydrology*, 601, 126643.

Srivastava, P.R., Sarkar, P. & Hanasusanto, G.A. (2023) A robust spectral clustering algorithm for sub-Gaussian mixture models with outliers. *Operations Research*, 71(1), 224–244.

Stagge, J.H., Tallaksen, L.M., Gudmundsson, L., Van Loon, A.F. & Stahl, K. (2015) Candidate distributions for climatological drought indices (SPI and SPEI). *International Journal of Climatology*, 35(13), 4027–4040.

Sun, C.X., Huang, G.H., Fan, Y., Zhou, X., Lu, C. & Wang, X.Q. (2019) Drought occurring with hot extremes: changes under future climate change on Loess Plateau, China. *Earths Future*, 7, 587–604.

Sung, J.H., Ryu, Y. & Chung, E.S. (2022) Multivariate frequency analysis for streamflow drought having different time

resolution using archimedean copula functions. *KSCE Journal of Civil Engineering*, 26(4), 2013–2021.

Wang, Z., Sun, S., Song, C., Wang, G., Lin, S. & Ye, S. (2022) Variation characteristics of high flows and their responses to climate change in permafrost regions on the Qinghai-Tibet Plateau, China. *Journal of Cleaner Production*, 376, 134369.

Watterson, I.G. (2005) Simulated changes due to global warming in the variability of precipitation, and their interpretation using a gamma-distributed stochastic model. *Advances in Water Resources*, 28(12), 1368–1381.

Wei, Y., Lu, H., Wang, J., Wang, X. & Sun, J. (2022) Dual influence of climate change and anthropogenic activities on the spatiotemporal vegetation dynamics over the Qinghai-Tibetan plateau from 1981 to 2015. *Earth's Futures*, 10(5), e2021EF002566.

Xavier, A.C.F., Martins, L.L., Rudke, A.P., de Morais, M.V.B., Martins, J.A. & Blain, G.C. (2022) Evaluation of Quantile Delta Mapping as a bias-correction method in maximum rainfall dataset from downscaled models in São Paulo state (Brazil). *International Journal of Climatology*, 42(1), 175–190.

Yang, X.L., Ren, L.L., Tong, R., Liu, Y., Cheng, X.R., Jiang, S.H. et al. (2015) Drought assessment and trends analysis from 20th century to 21st century over China. *Proceedings of the International Association of Hydrological Sciences*, 371(371), 89–94.

Yao, N., Li, L., Feng, P., Feng, H., Liu, D., Liu, Y. et al. (2020) Projections of drought characteristics in China based on a standardized precipitation and evapotranspiration index and multiple GCMs. *Science of the Total Environment*, 704, 135245.

Yoon, T. & Kang, D. (2023) Multi-modal stacking ensemble for the diagnosis of cardiovascular diseases. *Journal of Personalized Medicine*, 13(2), 373.

Yousaf, M., Ali, Z., Mohsin, M., Ilyas, M. & Shakeel, M. (2023) Development of a new hybrid ensemble method for accurate characterization of future drought using multiple global climate models. *Stochastic Environmental Research and Risk Assessment*, 37(12), 4567–4587.

Yuan, S., Zhao, K. & Xu, Z. (2023) Adaptive Gaussian mixture model for identifying outliers in historical route travel times. *IET Intelligent Transport Systems*, 17, 2458–2473.

Zhang, X., Hao, Z., Singh, V.P., Zhang, Y., Feng, S., Xu, Y. et al. (2022) Drought propagation under global warming: Characteristics, approaches, processes, and controlling factors. *Science of the Total Environment*, 838, 156021.

Zhang, Y., Li, M., Wang, S., Dai, S., Luo, L., Zhu, E. et al. (2021) Gaussian mixture model clustering with incomplete data. *ACM Transactions on Multimedia Computing, Communications, and Applications (TOMM)*, 17(1s), 1–14.

Zhu, B., Zhang, Z., Tian, J., Kong, R. & Chen, X. (2022b) Increasing negative impacts of climatic change and anthropogenic activities on vegetation variation on the Qinghai–Tibet Plateau during 1982–2019. *Remote Sensing*, 14(19), 4735.

Zhu, W., McBrearty, I.W., Mousavi, S.M., Ellsworth, W.L. & Beroza, G.C. (2022a) Earthquake phase association using a Bayesian Gaussian mixture model. *Journal of Geophysical Research: Solid Earth*, 127(5), e2021JB023249.

Zounemat-Kermani, M., Batelaan, O., Fadaee, M. & Hinkelmann, R. (2021) Ensemble machine learning paradigms in hydrology: a review. *Journal of Hydrology*, 598, 126266.

How to cite this article: Naz, R., Ali, Z., Kartal, V., Alshahrani, M. A., Hilali, S. O., & Al Samman, F. M. (2024). Improving drought monitoring using climate models with bias-corrected under Gaussian mixture probability models. *International Journal of Climatology*, 1–25. https://doi.org/10.1002/joc.8618